Separation Science and Technology
Publication details, including instructions for authors and subscription information:
http://www.informaworld.com/smpp/title~content=t713708471

The Instrument Spreading Correction in GPC. I. The General Shape Function Using a Linear Calibration Curve

Theodore Provder[ab]; Edward M. Rosen[a]
[a] MONSANTO COMPANY, ST. LOUIS, MISSOURI [b] SCM Corporation, Glidden-Durkee Division, Dwight P. Joyce Research Center, Strongsville, Ohio

To cite this Article Provder, Theodore and Rosen, Edward M.(1970) 'The Instrument Spreading Correction in GPC. I. The General Shape Function Using a Linear Calibration Curve', Separation Science and Technology, 5: 4, 437 — 484
To link to this Article: DOI: 10.1080/00372367008068442
URL: http://dx.doi.org/10.1080/00372367008068442

SEPARATION SCIENCE, 5(4), pp. 437–484, August, 1970

The Instrument Spreading Correction in GPC. I. The General Shape Function Using a Linear Calibration Curve*

THEODORE PROVDER† and EDWARD M. ROSEN
MONSANTO COMPANY
ST. LOUIS, MISSOURI 63166

Summary

A general shape function is proposed for describing the instrumental spreading behavior in gel permeation chromatography (GPC) columns due to axial dispersion and skewing effects. The general shape function contains statistical coefficients which describe the axial dispersion, skewing, and flattening of ideal monodisperse standards. A method denoted as the "method of molecular weight averages" is used to derive equations to correct GPC number- and weight-average molecular weights and intrinsic viscosities calculated from linear molecular weight calibration curves. The validity of these equations is experimentally verified with data for polystyrene, polybutadiene, and polyvinyl chloride polymers in tetrahydrofuran. The physical significance of the correction equations and their statistical coefficients is discussed in relation to the observed GPC chromatograms. Application of this shape function to the numerical Fourier analysis method for correcting differential molecular weight distribution (DMWD) curves is outlined. Also, a method is presented for obtaining corrected DMWD curves from a fitted molecular weight calibration curve corrected for instrument spreading by use of the hydrodynamic volume concept.

INTRODUCTION

Molecular weight distribution (MWD) curves calculated from gel permeation chromatograms are generally broader than the true or

* Presented at the ACS Symposium on Gel Permeation Chromatography, sponsored by the Division of Petroleum Chemistry at the 159th National Meeting of the American Chemical Society, Houston, Texas, February, 1970.

† Author to whom all correspondence should be addressed at: SCM Corporation, Glidden-Durkee Division, Dwight P. Joyce Research Center, 16651 Sprague Road, Strongsville, Ohio 44136.

absolute MWD curves due to instrumental spreading of the experimental chromatogram. Thus, the molecular weight averages calculated from the experimental chromatograms can be significantly different than the absolute molecular weight averages. The instrument spreading in gel permeation chromatography (GPC) has been attributed to axial dispersion (*1*) and skewing (*2*) effects. Several computational procedures (*1*, *3–10*) have been reported in the literature to correct for these effects. In each method a specific shape for the chromatogram of an ideal monodisperse species or narrow MWD sample is assumed. The use of a Gaussian shape function as in Tung's (*1*) basic method may be adequate when skewing effects are absent. The methods of Hess and Kratz (*4*), Smith (*3*), and Pickett, Cantow, and Johnson (*5*) attempt to correct for skewing effects. Duerksen and Hamielec (*2*) have shown that these methods are inadequate where overloading and interaction between species occur, particularly under conditions of high concentrations, high flow rate, and at high molecular weights. In addition these methods were subject to oscillations in the corrected chromatograms and differential molecular weight distribution curves (DMWD) because of the problem of distinguishing between the noise and the data in the chromatogram, particularly at the tails of the chromatogram.

Recently, Balke and Hamielec (*11*) used the number- and weight-average molecular weights to obtain empirical skewing operators to successfully correct molecular weight averages obtained from skewed chromatograms. Also, recently Tung (*12*) has illustrated the usefulness of the Fourier transform method for correcting observed chromatograms with a Gaussian instrument spreading function. In this paper a general statistical shape function is proposed for describing the instrumental spreading behavior in GPC columns and is applied to linear calibration curves by a method denoted as the "method of molecular weight averages." The use of this function with the Fourier transform method is touched on briefly and will be discussed extensively in Part II of this series. Also, a method is presented for obtaining corrected DMWD curves from a fitted calibration curve which has been corrected for instrument spreading by use of the hydrodynamic volume concept.

EXPERIMENTAL

Gel Permeation Chromatography

A Waters Associates Model 200 Gel Permeation Chromatograph, fitted with five Styragel columns having nominal porosity designations

of 10^6, 10^5, 10^4, 10^3, and 250 Å, was used for the analysis of molecular weight distributions. The average plate count of the columns at a solvent flow rate of 1 ml/min was 734 plates/foot with *o*-dichlorobenzene (ODCB). The columns were operated at room temperature, 24 ± 1°C, with Fisher Scientific Co. certified reagent grade THF (n_D^{25}, 0.888; bp, 64–66°C) used as the eluting solvent. The solvent contained 0.025 (w/v)% ditert-butyl-*p*-cresol which served as an antioxidant. The solvent flow rates were controlled at better than 1.00 ± 0.05 ml/min and 2.00 ± 0.05 ml/min. The degasser was operated at 55°C. The differential refractometer which had a 0.019 in. slit was operated on 8× and monitored the effluent streams at 42°C. To eliminate errors in elution volume measurement due to variations in the rate of solvent evaporation in the siphon tube (1 count = 5.003 ml at 1 ml/min, 1 count = 5.067 ml at 2 ml/min) a vapor feedback loop device, similar to that of Yau et al. (*13*), was installed. Samples were dissolved in degassed solvent taken from the GPC solvent reservoir and were filtered under N_2 pressure through 0.2 μ millipore filters. The samples were injected for 120 sec by means of the Waters Automatic Sample Injection System, ASIS. The variance in the reproducibility of chromatograms obtained from repetitive sample injections through the same loop was comparable to that obtained from repetitive sample injections between different loops. The GPC traces were digitally recorded at 20 sec intervals by means of the Waters Digital Curve Translator. Molecular weight averages, intrinsic viscosity, and normalized differential distribution curves were calculated on an IBM 360/65 computer according to the basic integral formulas given by Pickett et al. (*14*).

Calibration Standards

The calibration standards used were linear polystyrene standards (PS) from Pressure Chemical Co. (PC) and Waters Associates (W), linear polybutadiene standards (PBD) from Phillips Petroleum Co. (P), and linear polyvinyl chloride standards (PVC) from PC. The Waters Associates PS standards included some ultranarrow MWD recycle standards for which $\bar{M}_w/\bar{M}_n \leq 1.009$. The PS, PBD and PVC standards were injected via the ASIS at concentrations of 0.04, 0.05 and 0.075 (w/v) % respectively. The absolute number- and weight-average molecular weights and polydispersity ratios, designated respectively by $\bar{M}_n(t)$, $\bar{M}_w(t)$, and $P(t)$, and shown in Table 1, were those supplied by the vendor except where noted. The Mark-Houwink in-

TABLE 1

Absolute and Infinite Resolution Values of $\bar{M}_n$, $\bar{M}_w$, $[\eta]$, and P

Run	Standard	PEV	$10^{-3}\bar{M}_n(t)$	$10^{-3}\bar{M}_w(t)$	$[\eta](t)$	$P(t)$	$10^{-3}\bar{M}_n(\infty)$	$10^{-3}\bar{M}_w(\infty)$	$[\eta](\infty)$	$P(\infty)$
				Polystyrene, 1 ml/min						
180-175	PC-16A	40.15	0.578[a]	0.636	—	<1.1	0.521	0.632	—	1.21
180-176	PC-15A	38.20	1.21[a]	1.41	—	<1.16	1.20	1.57	—	1.31
180-177	PC-12A	37.50	1.73[a]	1.85	—	1.07	1.68	2.04	—	1.21
180-178	PC-11A	36.60	3.18[a]	3.53	0.0492	1.11	2.87	3.47	0.0496	1.21
180-179	W-4190042	34.55	9.70	10.3	0.106	1.06	7.86	9.59	0.103	1.22
180-180	W-4190039	33.25	19.65	19.85	0.172	1.01	16.01	18.67	0.163	1.17
180-181	W-4190041	31.09	49.0	51.0	0.331	1.04	—	—	—	—
180-182	W-41995	29.70	96.2	98.2	0.530	1.02	82.5	89.2	0.491	1.08
181-183	W-41984	28.50	164	173	0.781	1.06	139	161	0.747	1.15
181-184	NBS-705	28.30	170.9	179.3	0.802	1.049	144	178	0.797	1.232
181-185	NBS-706	27.85	136.5	257.8	1.006	1.889	119	284	1.052	2.377
181-186	W-4190037	26.25	392	411	1.441	1.05	271	407	1.417	1.50
181-187	PC-5A	25.60	404	507	1.568	1.26	348	531	1.713	1.53
181-188	W-490038	24.60	773	867	2.382	1.12	545	818	2.337	1.50
181-189	PC-14A	23.70	1610	1900	4.071	1.18	649	1160	2.964	1.79
181-190	W-61970	23.65	1780	2145	4.402	1.21	650	1147	2.944	1.77
184-207	W-27231	34.50	9.91	10.0[b]	0.107	<1.009	8.84	10.13	0.108	1.15
184-208	W-27232	33.45	16.35	16.5[b]	0.152	<1.009	14.31	15.63	0.144	1.09
184-209	W-27233	31.39	42.12	42.5[b]	0.296	<1.009	37.81	41.57	0.287	1.10
184-210	W-27234	29.65	95.14	96.0[b]	0.525	<1.009	82.94	90.18	0.495	1.09
184-211	W-27235	28.50	160.6	162[b]	0.760	<1.009	136.8	157.8	0.738	1.15
184-212	W-27231	34.51	9.91	10.0[b]	0.107	<1.009	8.92	10.25	0.109	1.15
184-213	W-27232	33.48	16.35	16.5[b]	0.152	<1.009	13.88	15.09	0.141	1.09
184-214	W-27233	31.42	42.12	42.5[b]	0.296	<1.009	38.03	41.45	0.287	1.09
				Polystyrene, 2 ml/min						
193-278	PC-16A	39.60	0.578[a]	0.636	—	<1.1	—	—	—	—
193-279	PC-15A	37.60	1.21[a]	1.41	—	<1.16	—	—	—	—

193-280	PC-12A	37.00	1.73[a]	1.85	—	1.07	1.75	2.12	—	1.23
193-281	PC-11A	35.90	3.18[a]	3.53	0.0492	1.11	2.93	3.62	0.0510	1.24
193-282	W-4190042	33.90	9.70	10.3	0.106	1.06	7.96	10.0	0.105	1.26
193-283	W-4190039	32.45	19.65	19.85	0.172	1.01	17.8	20.0	0.172	1.12
193-284	W-4190041	30.40	49.0	51.0	0.331	1.04	49.0	50.7	0.330	1.03
193-285	W-41995	28.95	96.2	98.2	0.530	1.02	90.4	100	0.541	1.11
194-286	W-41984	27.80	164	173	0.781	1.06	150	161	0.750	1.07
194-287	NBS-705	27.40	170.9	179.3	0.802	1.049	171	194	0.848	1.13
194-288	NBS-706	27.25	136.5	257.8	1.006	1.889	125	303	1.107	2.42
194-289	W-4190037	25.40	392	411	1.441	1.05	336	442	1.519	1.32
194-290	PC-5A	24.60	404	507	1.568	1.26	409	573	1.823	1.40
194-291	W-490038	23.80	773	867	2.382	1.12	853	880	2.477	1.03
194-292	PC-14A	23.10	1610	1900	4.071	1.18	834	1140	2.963	1.37
194-293	W-61970	23.00	1780	2145	4.402	1.21	924	1170	3.02	1.27
				Polybutadiene,[c] 1 ml/min						
159-045	P-17M	32.01	16.1	17.0	—	1.06	12.4	18.3	—	1.64
159-046	P-170M	27.16	135	170	—	1.26	89.1	149	—	1.68
159-047	P-272M	26.10	206	272	—	1.32	145	303	—	2.09
159-048	P-332M	25.80	226	332	—	1.47	132	401	—	3.05
159-049	P-432M	25.22	286	432	—	1.48	127	493	—	3.88
				Polyvinyl Chloride, 1 ml/min						
158-042	PC-V2	30.80	25.5	68.6	0.70	2.69	24.0	59.9	0.74	2.50
158-043	PC-V3	29.70	41.1	118	1.13	2.87	38.8	95.5	1.06	2.46
159-044	PC-V4	29.31	54.0	132	1.25	2.44	45.9	114	1.21	2.48

[a] The $\bar{M}_n(t)$ value used were those determined by Wachter and Simon (*32*) with an extended range vapor pressure osmometer. $\bar{M}_w(t)$ values were determined from the $\bar{M}_n(t)$ values and the vendor supplied $P(t)$ values.

[b] The $\bar{M}_w(t)$ values for the recycle PS-standards were read off the molecular weight calibration curve associated with the PEV. $\bar{M}_n(t)$ values were determined from the $\bar{M}_w(t)$ values and the vendor supplied $P(t)$ values.

[c] The ranges in per cent geometrical isomer content of the PBD-standards varied as follows: $43.5 \leq cis \leq 51.7$, $41.7 \leq trans \leq 49.1$ and $6.6 \leq$ vinyl ≤ 8.4.

trinsic viscosity-molecular weight relations used to obtain $[\eta](t)$ for PVC (*15*) and PS were, respectively,

$$[\eta]^{\text{PVC}}_{\text{THF},25°\text{C}} = 1.63 \times 10^{-4}\, \bar{M}_v^{0.766} \qquad 20{,}000 < \bar{M}_v < 170{,}000 \qquad (1)$$

and

$$[\eta]^{\text{PS}}_{\text{THF},25°\text{C}} = 1.60 \times 10^{-4}\, \bar{M}_v^{0.706} \qquad \bar{M}_v > 3000 \qquad (2)$$

Equation (2) was obtained via least-squares analysis of data supplied by ArRo Laboratories (*16*).

The calibration curves for PS and PBD standards were obtained by associating peak elution volume (PEV) with $\bar{M}_w$, while for the broad

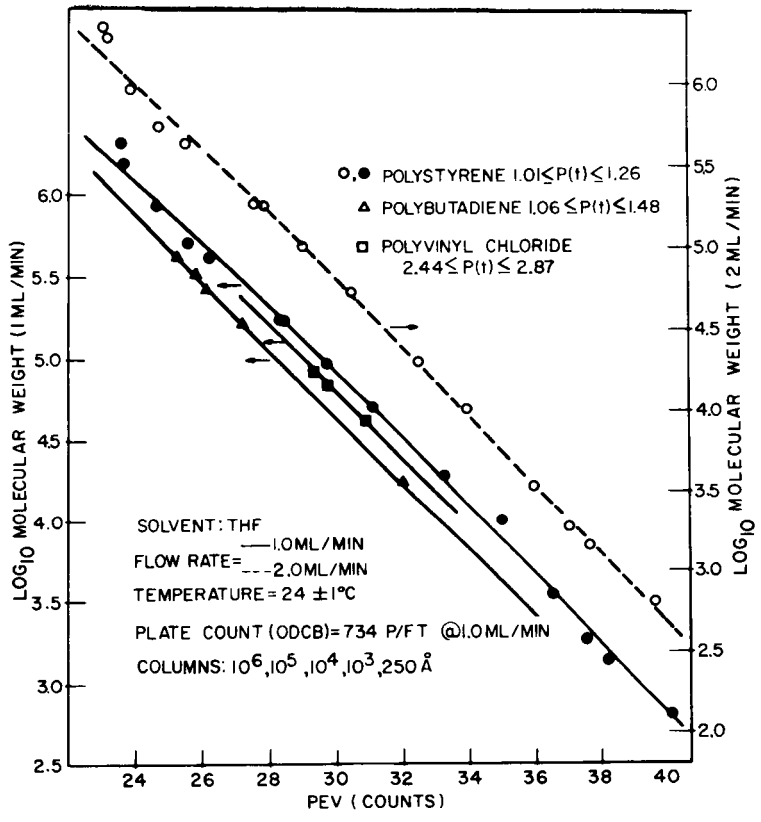

FIG. 1. Molecular weight calibration curves for polystyrene, polybutadiene, and polyvinyl chloride.

TABLE 2

Absolute and Infinite Resolution Values of $\bar{M}_n$, $\bar{M}_w$, $[\eta]$, and P

Run	Wt% composition[a]	$10^{-3}\bar{M}_n(t)$[b]	$10^{-3}\bar{M}_w(t)$	$[\eta](t)$	$P(t)$	$10^{-3}\bar{M}_n(\infty)$	$10^{-3}\bar{M}_w(\infty)$	$[\eta](\infty)$	$P(\infty)$
		Polystyrene Blends, Flow Rate = 2 ml/min							
196-302-2	0/50/50	64.9	74.6	0.431	1.11	61.9	73.7	0.428	1.19
196-303-2	50/50/0	28.1	35.4	0.252	1.24	26.9	36.8	0.258	1.37
196-304-2	50/0/50	32.6	59.0	0.351	1.79	30.6	61.8	0.363	2.02
196-305-2	75/25/0	23.1	27.6	0.212	1.18	21.8	29.2	0.219	1.34
196-306-2	25/75/0	35.6	43.2	0.291	1.18	34.3	42.6	0.289	1.24
196-307-2	33.3/33.3/33.3	36.7	56.3	0.344	1.51	34.6	56.9	0.347	1.65
196-308-2	16.7/33.3/50	48.8	69.4	0.404	1.42	47.1	70.5	0.409	1.50
196-309-2	50/33.3/16.7	29.4	43.3	0.285	1.45	27.8	44.4	0.290	1.60

[a] The wt% of each polystyrene standard in the mixture refers to the standards in the following order: W-4190039, W-4190041, and W-41995.

[b] The absolute values $\bar{M}_n(t)$, $\bar{M}_w(t)$, and $[\eta](t)$ of the blends were calculated from the absolute values of the individual components and the compositions of the blends.

PVC standards PEV was associated with $(\bar{M}_n \cdot \bar{M}_w)^{1/2}$. The number- and weight-average molecular weights, intrinsic viscosity, and polydispersity ratios calculated from the molecular weight calibration curves (shown in Fig. 1), assuming perfect or infinite resolution, are designated as $\bar{M}_n(\infty)$, $\bar{M}_w(\infty)$, $[\eta](\infty)$, and $P(\infty)$, and are listed in Table 1.

Polystyrene Blends

Some polystyrene blends composed of varying amounts of samples W-4190039, W-4190041, and W-41995 having a polydispersity range of $1.11 \leq P(t) \leq 1.79$ were injected via the ASIS at 0.04 (w/v)% for 120 sec. These samples were run through the columns at 2.00 ± 0.05 ml/min. The compositions of the blends and absolute and infinite resolution values of $\bar{M}_n$, $\bar{M}_w$, $[\eta]$, and P are shown in Table 2. The baseline adjusted raw chromatograms of these multimodal polystyrene blends are shown in Figs. 2 and 3.

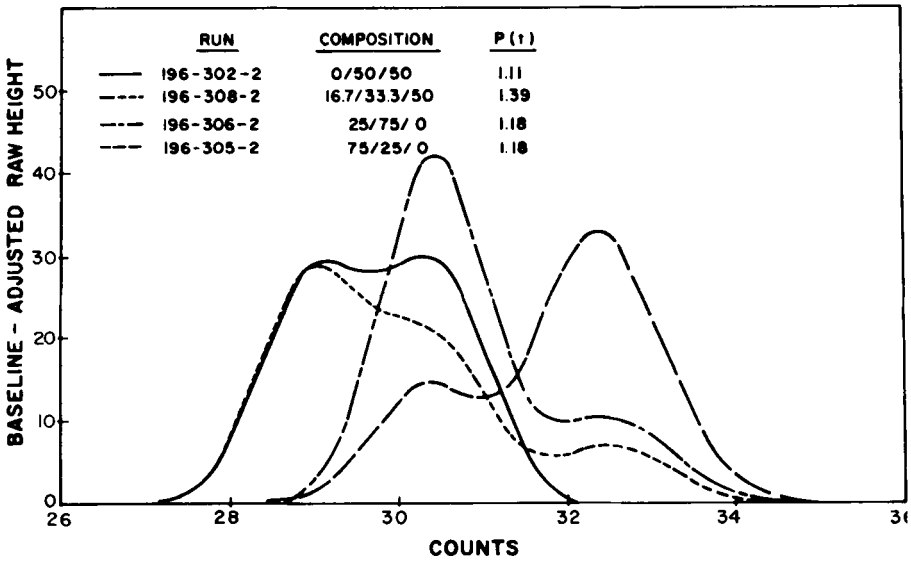

FIG. 2. Baseline-adjusted raw chromatograms of some polystyrene blends of samples W-4190039, W-4190041, and W-41995 at a flow rate of 2 ml/min.

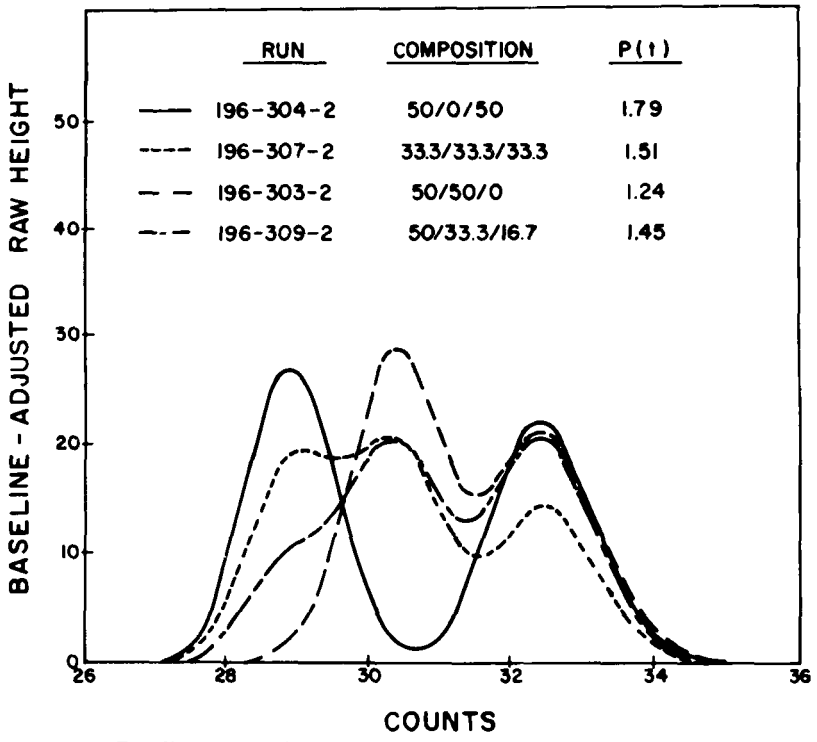

FIG. 3. Baseline-adjusted raw chromatogram of some polystyrene blends of samples W-4190039, W-4190041, and W-41995 at a flow rate of 2 ml/min.

THEORY

Method of Molecular Weight Averages

Tung (*1*) has shown that the normalized* observed GPC chromatogram, $F(v)$, at elution volume v is related to the normalized GPC chromatogram corrected for instrumental broadening, $W(v)$, by means of the shape function $G(v)$ through the relation

$$F(v) = \int_{-\infty}^{\infty} G(v - y)W(y)\,dy \tag{3}$$

The kth molecular weight average associated with the corrected chro-

* The word "normalized" means that the area of the observed chromatogram is unity.

matogram is denoted by $M_k(t)$ (true or absolute value), and the kth molecular weight average associated with the observed chromatogram is denoted by $M_k(\infty)$ assuming perfect or infinite resolution. Then, the ratio $M_k(t)/M_k(\infty)$ is given by

$$\frac{M_k(t)}{M_k(\infty)} = \frac{\int_{-\infty}^{\infty} W(v)M(v)^{k-1}\,dv \Big/ \int_{-\infty}^{\infty} W(v)M(v)^{k-2}\,dv}{\int_{-\infty}^{\infty} F(v)M(v)^{k-1}\,dv \Big/ \int_{-\infty}^{\infty} F(v)M(v)^{k-2}\,dv} \tag{4}$$

where $k = 1, 2, 3, 4$ corresponds to the number-, weight-, Z- and $Z + 1$-average molecular weight, respectively.

A similar expression can be written for the ratio of the intrinsic viscosity associated with the corrected chromatogram, $[\eta](t)$, to the intrinsic viscosity associated with the observed chromatogram, $[\eta](\infty)$, assuming infinite resolution. This expression is given by

$$\frac{[\eta](t)}{[\eta](\infty)} = \int_{-\infty}^{\infty} W(v)M(v)^{\epsilon}\,dv \Big/ \int_{-\infty}^{\infty} F(v)M(v)^{\epsilon}\,dv \tag{5}$$

where ϵ is the exponent in the Mark-Houwink intrinsic viscosity-molecular weight expression.

For calibration curves which are linear in $\log_{10} M$ or curves which are linear in $\log_{10} M$ over the elution volume range of interest

$$M(v) = D_1 \exp(-D_2 v) \tag{6}$$

where $D_1, D_2 > 0$. Substituting Eq. (6) into (4) and (5) yields the following relations

$$\frac{M_k(t)}{M_k(\infty)} = \frac{\bar{W}[D_2(k-1)]/\bar{W}[D_2(k-2)]}{\bar{F}[D_2(k-1)]/\bar{F}[D_2(k-2)]} \tag{7}$$

$$\frac{[\eta](t)}{[\eta](\infty)} = \bar{W}[D_2\epsilon]/\bar{F}[D_2\epsilon] \tag{8}$$

where $\bar{W}$ and $\bar{F}$ are the bilaterial Laplace transforms of $W(v)$ and $F(v)$, respectively, and the square brackets indicate functionality. The general bilateral Laplace transform of $F(v)$ can be written as

$$\bar{F}(s) = \int_{-\infty}^{\infty} \exp(-sv) \left[\int_{-\infty}^{\infty} G(v-y)W(y)\,dy \right] dv \tag{9}$$

Application of the convolution theorem of the bilateral Laplace transform leads to

$$\bar{F}(s) = \bar{W}(s)\bar{G}(s) \tag{10}$$

The ratio of the absolute to infinite resolution molecular weight averages and intrinsic viscosity becomes

$$\frac{M_k(t)}{M_k(\infty)} = \tilde{G}[D_2(k-2)]/\tilde{G}[D_2(k-1)] \tag{11}$$

$$\frac{[\eta](t)}{[\eta](\infty)} = 1/\tilde{G}[D_{2\epsilon}] \tag{12}$$

where

$$\tilde{G}(s) = \int_{-\infty}^{\infty} \exp[-s(v-y)]G(v-y)\,d(v-y) \tag{13}$$

and $G(v-y)$ is the general instrument spreading function defined in Eqs. (14) and (15).

The Instrument Spreading Shape Function

Tung (*1*) has used a Gaussian function to describe the instrumental spreading. This shape function is inadequate when skewing effects are present. Smith's (*3*) use of a log-normal shape function is not of sufficient generality to account for skewing and has not been successful (*2*). The method of Pickett and co-workers (*5*), which uses the chromatogram shapes of narrow MWD standards, has been only partially successful since it overcorrects for skewing (*2*). The need for a non-Gaussian shape function has been empirically demonstrated rather extensively by Hamielec and co-workers (*2*, *11*). Skewed chromatograms are produced under conditions of high flow rate (short residence times), increased viscosity due to high-molecular weight species, and/or column overloading as well as loss of resolution at the high- or low-molecular weight ends of the calibration curve.

A general normalized statistical shape function describing the instrumental broadening behavior in GPC columns is proposed and has the form

$$G(v-y) = G_T(v-y) + \sum_{n=3}^{\infty} \{(-1)^n A_n \mu^{n/2} G_T^n(v-y)/n!\} \tag{14}$$

where $G_T(v-y)$ and $G_T^n(v-y)$ denote the normal form of the Gaussian instrumental spreading function first used by Tung (*1*),

$$G_T(v-y) = (1/2\pi\mu_2)^{1/2} \exp[-(v-y)^2/2\,\mu_2] \tag{15}$$

and its nth order derivatives with respect to v, respectively.

The coefficients A_n are functions of μ_n, the nth order moments about

the elution volume y of the instrument spreading function. The first two coefficients are of direct statistical significance and are

$$A_3 = \mu_3/\mu^{3/2} \tag{16}$$

$$A_4 = (\mu_4/\mu_2^2 - 3) \tag{17}$$

where the variance μ_2 is related to the resolution factor h by the relation

$$\mu_2 = 1/h \tag{18}$$

The resolution factor h defined by Eqs. (15) and (18) is equal to two times the resolution factor defined in the original Tung (*1*) formulation. In the limiting case of an ideal monodisperse standard or ultranarrow MWD standard for which $P(t) = 1$, the moments μ_n are also the nth order moments about the mean of the normalized observed GPC chromatogram.

The coefficient A_3 provides an absolute statistical measure of skewness. When $A_3 = 0$, the chromatogram of the ideal monodisperse standard is symmetrical about the elution volume y. When $A_3 > 0$, the chromatogram of the ideal standard has a long tail at high elution volumes and is skewed to high elution volumes or low molecular weights; and when $A_3 < 0$, the chromatogram has a long tail at low elution volumes and is skewed to low elution volumes or high molecular weights.

The coefficient A_4 provides a statistical measure of the flattening or kurtosis of the chromatogram of the ideal monodisperse standard and is related to instrumental broadening effects due to skewing and axial dispersion. The kurtosis coefficient measures the excess flatness or thinness of the chromatogram peak compared to that of a Gaussian curve. When $A_4 = 0$, the chromatogram is Gaussian in shape. When $A_4 > 0$, the chromatogram is leptokurtic, taller and slimmer than the Gaussian curve. When $A_4 < 0$, the normalized observed chromatogram is platykurtic, flatter or squat at the center of the curve than the corresponding Gaussian curve.

In principle, the coefficients A_n can be obtained from the moments about the mean elution volume of the normalized observed chromatograms of narrow MWD standards. However, the narrow MWD standards may have some natural skewness, flatness, and dispersion associated with their MWD's, and the computation of μ_3 and higher moments may be subject to large numerical errors. Furthermore, it is desirable to consider the coefficients A_n as parameters which can be mathematically manipulated. The coefficients A_n are functions of elution volume, but will be considered to be constant or slowly varying functions of elution

volume in the integration in Eq. (13). In order to obtain the contributions to the coefficients A_n due solely to instrumental broadening, expressions will be derived for $\bar{M}_n(t)$, $\bar{M}_w(t)$, and $[\eta](t)$ in terms of h, μ_3, and μ_4. Subsequently, the values of h, μ_3, and μ_4 will be determined by fitting these expressions to the experimental values of $\bar{M}_n(t)$, $\bar{M}_w(t)$, and $[\eta](t)$.

The coefficients A_5 and higher are functions of higher order moments and/or products of lower order A_n coefficients. The higher order moments do not have a simple geometrical interpretation. The higher even order moments are further measures of dispersion or flatness and the higher odd order moments are further measures of skewness. A complete derivation of the general statistical shape function describing deviations from ideal Gaussian behavior by means of moment generating and cumulant generating functions has been described by Aitken (*17*) and others (*18*, *19*, *22*).

Evaluation of $M_k(t)/M_k(\infty)$ and $[\eta](t)/[\eta](\infty)$

The bilateral Laplace transform of $G(v - y)$ in reduced variable notation is

$$\bar{G}(s/\sqrt{h}) = \int_{-\infty}^{\infty} \exp(-sx/\sqrt{h})G(x)\,dx \tag{19}$$

where $x = (v - y)/\sqrt{\mu_2} = \sqrt{h}(v - y)$. The evaluation of Eq. (19) can be conveniently carried out by expressing the integrand in terms of Hermite polynomials. Using the relations (*20*)

$$\begin{aligned} H_n(x) &= (-1)^n\phi^n(x)/\phi(x) \\ \phi(x) &= (1/2\pi)^{1/2}\exp(-x^2/2) \end{aligned} \tag{20}$$

in conjunction with Eqs. (14) and (15), the general shape function becomes

$$G(x) = \phi(x)\left[1 + \sum_{n=3}^{\infty}(A_n/n!)H_n(x)\right] \tag{21}$$

The form of the general shape function in Eq. (21) is known as the Gram-Charlier series (*21–23*). Through the use of the generating function (*20*) for Hermite polynomials, the exponential term in the integrand of Eq. (19) becomes

$$\exp(-sx/\sqrt{h}) = \exp(s^2/2h)\sum_{m=0}^{\infty}(H_m(x)/m!)(-s/\sqrt{h})^m \tag{22}$$

Substitution of Eqs. (21) and (22) into Eq. (19) leads to

$$\bar{G}(s/\sqrt{h}) = \exp(s^2/2h)\left\{\sum_{m=0}^{\infty}(s/\sqrt{h})^m(1/m!)\left(\int_{-\infty}^{\infty}\phi(x)H_m(x)H_0(x)\,dx\right)\right.$$
$$\left.+\sum_{n=0}^{\infty}\sum_{m=3}^{\infty}(A_n/n!m!)(-s\sqrt{h})^m\left(\int_{-\infty}^{\infty}\phi(x)H_m(x)H_0(x)\,dx\right)\right\} \quad (23)$$

Using the orthonormality conditions (*20*) for Hermite functions,

$$\int_{-\infty}^{\infty}\phi(x)H_n(x)H_m(x)\,dx = \begin{matrix} n! \\ 0 \end{matrix}\Bigg\} \begin{matrix} n = m \\ n \neq m \end{matrix} \quad (24)$$

in Eq. (23) yields the following expression,

$$\bar{G}(s/\sqrt{h}) = \exp(s^2/2h)\left\{1+\sum_{n=3}^{\infty}(A_n/n!)(s/\sqrt{h})^n\right\} \quad (25)$$

Substitution of the expression for $\bar{G}(s)$ into Eqs. (11) and (12) yields

$$\frac{M_k(t)}{M_k(\infty)} = \exp\left[\frac{-D_2^2(2k-3)}{2h}\right]\frac{\left\{1+\sum_{n=3}^{\infty}\left(\frac{A_n}{n!}\right)\left(\frac{-D_2(k-2)}{\sqrt{h}}\right)^n\right\}}{\left\{1+\sum_{n=3}^{\infty}\left(\frac{A_n}{n!}\right)\left(\frac{-D_2(k-1)}{\sqrt{h}}\right)^n\right\}} \quad (26)$$

$$\frac{[\eta](t)}{[\eta](\infty)} = \exp\left[\frac{-\epsilon D_2^2}{2h}\right]\Bigg/\left\{1+\sum_{n=3}^{\infty}\left(\frac{A_n}{n!}\right)\left(\frac{-\epsilon D_2}{\sqrt{h}}\right)^n\right\} \quad (27)$$

Truncation of the Gram-Charlier series in Eq. (21) leads to the Edgeworth series (*24*), where $A_5 = 0$, $A_6 = 10A_3^2$ and $A_n = 0$ for $n > 7$. Expressions for $\bar{M}_n(t)$, $\bar{M}_w(t)$, and $[\eta](t)$ may be written in terms of the fundamental parameters h, μ_3, and μ_4 as follows:

$$\bar{M}_n(t) = \bar{M}_n(\infty)\exp(D_2^2/2h)\left\{1+\frac{D_2^3\mu_3}{6}+\frac{D_2^4}{24}\left(\mu_4-\frac{3}{h^2}\right)+\frac{1}{2}\left(\frac{D_2^3\mu_3}{6}\right)^2\right\} \quad (28)$$

$$\bar{M}_w(t) = \bar{M}_w(\infty)\exp(-D_2^2/2h)\Bigg/\left\{1-\frac{D_2^3\mu_3}{6}+\frac{D_2^4}{24}\left(\mu_4-\frac{3}{h^2}\right)+\frac{1}{2}\left(\frac{D_2^3\mu_3}{6}\right)^2\right\} \quad (29)$$

$$[\eta](t) = [\eta](\infty)\exp(-\epsilon^2D_2^2/2h)\Bigg/\left\{1-\frac{\epsilon^3D_2^3\mu_3}{6}\right.$$

$$+ \frac{\epsilon^4 D_2^4}{24}\left(\mu_4 - \frac{3}{h^2}\right) + \frac{1}{2}\left(\frac{\epsilon^3 D_2^3 \mu_3}{6}\right)^2\Bigg\} \quad (30)$$

DETERMINATION OF h, μ_3, AND μ_4 FROM STANDARDS

$\bar{M}_n$, $\bar{M}_w$ Supplied

If the coefficients of the Mark-Houwink intrinsic viscosity-molecular weight relationship are unavailable, then only $\bar{M}_n(t)$ and $\bar{M}_w(t)$ can be used to determine h and μ_3 in Eqs. (28) and (29). If we denote the ratios $\bar{M}_n(t)/\bar{M}_n(\infty)$ and $\bar{M}_w(\infty)/\bar{M}_w(t)$ as $R_n(t,\infty)$ and $R_w(\infty,t)$, respectively, Eqs. (28) and (29) can be combined to yield

$$[R_n(t,\infty) - R_w(\infty,t)] \exp(-D_2^2/2h) = 2[D_2^3\mu_3/6] \quad (31)$$

$$[R_n(t,\infty) + R_w(\infty,t)] \exp(-D_2^2/2h) = 2\left[1 + \frac{D_2^4}{24}\left(\mu_4 - \frac{3}{h^2}\right) + \frac{1}{2}\left(\frac{D_2^3\mu_3}{6}\right)^2\right] \quad (32)$$

If

$$\frac{D_2^4}{24}\left(\mu_4 - \frac{3}{h^2}\right) + \frac{1}{2}\left[\frac{D_2^3\mu_3}{6}\right]^2 \ll 1 \quad (33)$$

Eqs. (31) and (32) can be combined to give simple algebraic expressions for h and μ_3 as follows:

$$h = \left(\frac{D_2^2}{2}\right) \Big/ \log_e\left\{\frac{[R_n(t,\infty) + R_w(\infty,t)]}{2}\right\} \quad (34)$$

$$\mu_3 = \left(\frac{6}{D_2^3}\right)\left\{\frac{R_n(t,\infty) - R_w(\infty,t)}{R_n(t,\infty) + R_w(\infty,t)}\right\} \quad (35)$$

A calibration curve for h and μ_3 as functions of PEV can be obtained from standards via Eqs. (34) and (35). The corrected number- and weight-average molecular weights and intrinsic viscosity of other samples (provided the Mark-Houwink constants are known), which shall be designated as $\bar{M}_n(h,\mu_3)$, $\bar{M}_w(h,\mu_3)$, and $[\eta](h,\mu_3)$, respectively, can be obtained from

$$\bar{M}_n(h,\mu_3) = \bar{M}_n(\infty) \exp(D_2^2/2h)\{1 + D_2^3\mu_3/6\} \quad (36)$$

$$\bar{M}_w(h,\mu_3) = \bar{M}_w(\infty) \exp(-D_2^2/2h)\{1 - D_2^3\mu_3/6\}^{-1} \quad (37)$$

$$[\eta](h,\mu_3) = [\eta](\infty) \exp(-\epsilon^2 D_2^2/2h)\{1 - \epsilon_2^3 D_2^3\mu_3/6\}^{-1} \quad (38)$$

In using Eqs. (34) through (38), it is important to be certain that Eq. (33) holds so that terms in D_2^4 or higher can be neglected.

When $D_2^3\mu_3/6 \ll 1$, the term in braces in Eq. (37) can be expanded to give the same term that appears in braces in Eq. (36). Under this condition, Eqs. (36) and (37) then become equivalent to the empirical correction equations obtained by Balke and Hamielec (*11*). Their empirical skewing operator sk and resolution factor h' are then related to μ_3 and h, respectively, according to the relations

$$\begin{aligned} sk &= D_2^3\mu_3/3 \\ h' &= h/2 \end{aligned} \tag{39}$$

$\bar{M}_n$, $[\eta]$ Supplied

The measurement of the weight-average molecular weight by light-scattering techniques is a time consuming and often experimentally difficult task compared to the determination of the number-average molecular weight by membrane or vapor pressure osmometry. When $\bar{M}_n$ and $[\eta]$ are relatively easy to obtain, compared to $\bar{M}_w$, and the Mark-Houwink coefficients are available, Eqs. (28) and (30) can be used to obtain h and μ_3.

Upon denoting the ratio $[\eta](\infty)/[\eta](t)$ as $R_v(\infty,t)$, Eqs. (28) and (30) can be combined to yield

$$R_n(t,\infty)\exp(-D_2^2/2h) - R_v(\infty,t)\exp(-\epsilon^2D_2^2/2h) = \mu_3D_2^3(1+\epsilon^3)/6 \tag{40}$$

$$R_n(t,\infty)\exp(-D_2^2/2h) + R_v(\infty,t)\exp(-\epsilon^2D_2^2/2h) - 2 = \mu_3D_2^3(1-\epsilon^3)/6 \tag{41}$$

where again terms in D_2^4 and D_2^6 have been neglected. Manipulation of Eqs. (40) and (41) leads to the following expression for h

$$h = \left(\frac{D_2^2}{2}\right) \Big/ \log_e\left[\frac{\epsilon^3R_n(t,\infty)}{(1+\epsilon^3) + R_v(\infty,t)[1-(\epsilon^2D_2^2/2h)]}\right] \tag{42}$$

A value for h can be rapidly obtained from Eq. (42) by an iterative procedure with a desk calculator. A good initial guess is obtained by setting the term $(\epsilon^2D_2^2/4h)$ to zero. Then, the guessed value is inserted into Eq. (42) and a new value computed. This procedure is continued until there is satisfactory agreement between two successively calculated values of h. Once h is obtained, μ_3 can be readily obtained from either Eq. (40) or (41). Then, the corrected number- and weight-average molecular weights and intrinsic viscosity of other samples can be obtained from Eqs. (36) through (38).

$\bar{M}_n$, $\bar{M}_w$, $[\eta]$ Supplied

When values of the absolute number- and weight-average molecular weights and intrinsic viscosity are available, h, μ_3, and μ_4 can be obtained from Eqs. (28), (29), and (30) by solving for them with the aid of an "algorithm for least squares estimation of nonlinear parameters" and a computer. When the values of h obtained in this manner are large, $h > 2.0$, the exponential factor in $D_2^2/2h$ approaches unity and can be neglected. Then, the corrected number- and weight-average molecular weights and intrinsic viscosities can be obtained from the following equations

$$\bar{M}_n(\mu_3,\mu_4) = \bar{M}_n(\infty)\left\{1 + \frac{D_2^3\mu_3}{6} + \frac{D_2^4\mu_4}{24} + \frac{1}{2}\left(\frac{D_2^2\mu_3}{6}\right)^2\right\} \tag{43}$$

$$\bar{M}_w(\mu_3,\mu_4) = \bar{M}_w(\infty)\left\{1 - \frac{D_2^3\mu_3}{6} + \frac{D_2^4\mu_4}{24} + \frac{1}{2}\left(\frac{D_2^3\mu_3}{6}\right)^2\right\}^{-1} \tag{44}$$

$$[\eta](\mu_3,\mu_4) = [\eta](\infty)\left\{1 - \frac{\epsilon^3 D_2^3\mu_3}{6} + \frac{\epsilon^4 D_2^4\mu_4}{24} + \frac{1}{2}\left(\frac{\epsilon^3 D_2^3\mu_3}{6}\right)^2\right\}^{-1} \tag{45}$$

DISCUSSION OF THE EFFECTS OF h, μ_3, AND μ_4 ON $\bar{M}_n(\infty)$, $\bar{M}_w(\infty)$, AND $[\eta](\infty)$

The effect that skewed GPC chromatograms have upon calculated number- and weight-average molecular weights and intrinsic viscosity is graphically illustrated in Fig. 4. The correction Eqs. (28), (29), and (30) have been plotted as a function of μ_3 for the situation where axial dispersion is absent, $h = \infty$ and $\mu_4 = 0$. Typical experimental values have been assigned to D_2 and ϵ, $D_2 = 0.5$ and $\epsilon = 0.7$.

Positive values of μ_3 indicate that the chromatogram is skewed to high elution volumes (low molecular weight). As a result, $\bar{M}_n(\infty)$ always will be less than the true value, $\bar{M}_n(\mu_3)$. As μ_3 increases, the correction necessary to raise $\bar{M}_n(\infty)$ to $\bar{M}_n(\mu_3)$ monotonically increases. $\bar{M}_w(\infty)$ is less than the true value, $\bar{M}_w(\mu_3)$, in the range $0 < \mu_3 < 12/D_2^3$. As μ_3 increases, the correction necessary to raise $\bar{M}_w(\infty)$ to $\bar{M}_w(\mu_3)$ at first increases monotonically. At $\mu_3 = 6/D_2^3$ the correction reaches a maximum value $[\bar{M}_w(\mu_3)/\bar{M}_w(\infty) = 2]$ and then decreases monotonically. When $\mu_3 > 12D_2^3$, $\bar{M}_w(\infty) > \bar{M}_w(\mu_3)$ and the correction necessary to lower $\bar{M}_w(\infty)$ to $\bar{M}_w(\mu_3)$ increases in a monotonic fashion. This unusual behavior is due to the effect of the quadratic term in μ_3 in Eq. (29). Large values of μ_3, $\mu_3 > 15$, are due to a loss of resolution at high molecular weights. The high molecular weight species are not adequately frac-

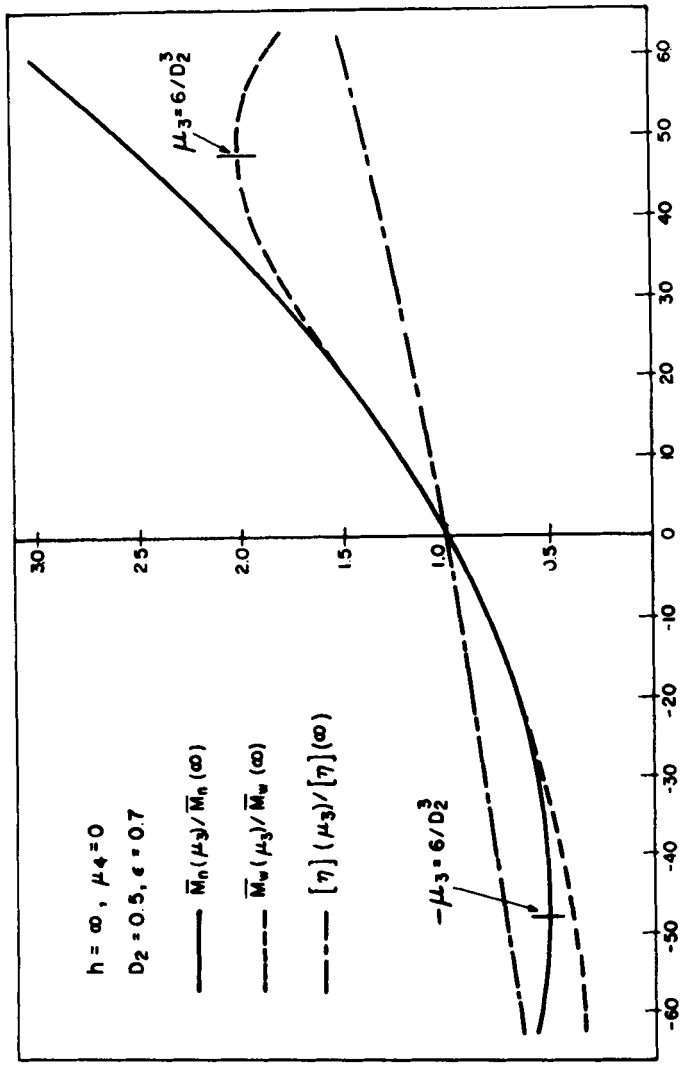

FIG. 4. Correction factor curves for $\bar{M}_n$, $\bar{M}_w$, and $[\eta]$ vs μ_3 for $h = \infty$ and $\mu_4 = 0$.

tionated by the gel and tend to elute over a very narrow range of elution volumes. This effect causes the chromatogram to be extremely skewed toward higher elution volumes and causes the calibration curve to tail up sharply at high molecular weights.

Negative values of μ_3 indicate that the chromatogram is skewed to low elution volumes (high molecular weight). This is due to a loss of resolution at low molecular weights and is associated with a sharp downturn in the calibration curve at high elution volumes. Thus, for all negative values of μ_3, $\bar{M}_w(\infty) > \bar{M}_w(\mu_3)$ and the correction necessary to lower $\bar{M}_w(\infty)$ to $\bar{M}_w(\mu_3)$ increases in a monotonic fashion. Because of the quadratic term in μ_3 in Eq. (28), $\bar{M}_n(\infty) > \bar{M}_n(\mu_3)$ for $-12/D_2^3 < \mu_3 < 0$ and $\bar{M}_n(\infty) < \bar{M}_n(\mu_3)$ for $\mu_3 < -12/D_2^3$. As μ_3 decreases, the correction necessary to lower $\bar{M}_n(\infty)$ to $\bar{M}_n(\mu_3)$ at first increases monotonically. At $\mu_3 = -6/D_2^3$ the correction reaches a maximum value $[\bar{M}_n(\mu_3)/\bar{M}_n(\infty) = 0.5]$ and then decreases monotonically. For $\mu_3 < -12/D_2^3$ the correction to raise $\bar{M}_n(\infty)$ to $\bar{M}_n(\mu_3)$ increases in a monotonic fashion.

The empirically defined skewing operator, sk, of Balke and Hamielec (*11*) has the effect of raising $\bar{M}_n(\infty)$ and lowering $\bar{M}_w(\infty)$ equally through their correction equations, which as previously mentioned are limiting cases of Eqs. (36) and (37),

$$\bar{M}_n(t) = \bar{M}_n(\infty) \exp(D_2^2/4h')[1 + \tfrac{1}{2}sk] \quad (46)$$

$$\bar{M}_w(t) = \bar{M}_w(\infty) \exp(-D_2^2/4h')[1 + \tfrac{1}{2}sk] \quad (47)$$

These equations are based on the assumption that the main effect of the skewing correction is to shift the intercept of the molecular weight calibration curve. Figure 4 shows that this assumption is only valid for a narrow range of μ_3 values, and thus a narrow range of elution volumes. For $D_2 = 0.5$, $\bar{M}_n(t)/\bar{M}_n(\infty) \simeq \bar{M}_w(t)/\bar{M}_w(\infty)$ only in the range $-15 \leq \mu_3 \leq 15$, $-0.625 \leq sk \leq 0.625$.

The behavior of $[\eta](\infty)$ as a function of μ_3 parallels that of $\bar{M}_w(\infty)$, except that the ϵ-parameter in Eq. (30) damps out the effect of the quadratic term in μ_3 over the range of μ_3 which is of practical interest.

The separate effect of h ($\mu_3 = \mu_4 = 0$) and μ_4 ($h = \infty$, $\mu_3 = 0$), upon $\bar{M}_n(\infty)$, $\bar{M}_w(\infty)$, and $[\eta](\infty)$ are shown in Fig. 5 for $D_2 = 0.5$ and $\epsilon = 0.7$. It can be seen that h raises $\bar{M}_n(\infty)$ and lowers $\bar{M}_w(\infty)$ and $[\eta](\infty)$ to their respective values $\bar{M}_n(h)$, $\bar{M}_w(h)$, and $[\eta](h)$. $\bar{M}_n(\infty)$ is raised and $\bar{M}_w(\infty)$ is lowered by the same amount for $h > 1.00$. For $h < 1.00$ and $D_2 = 0.5$, the effects of axial dispersion although symmetric in elution volume space do not shift the DMWD curve of narrow MWD

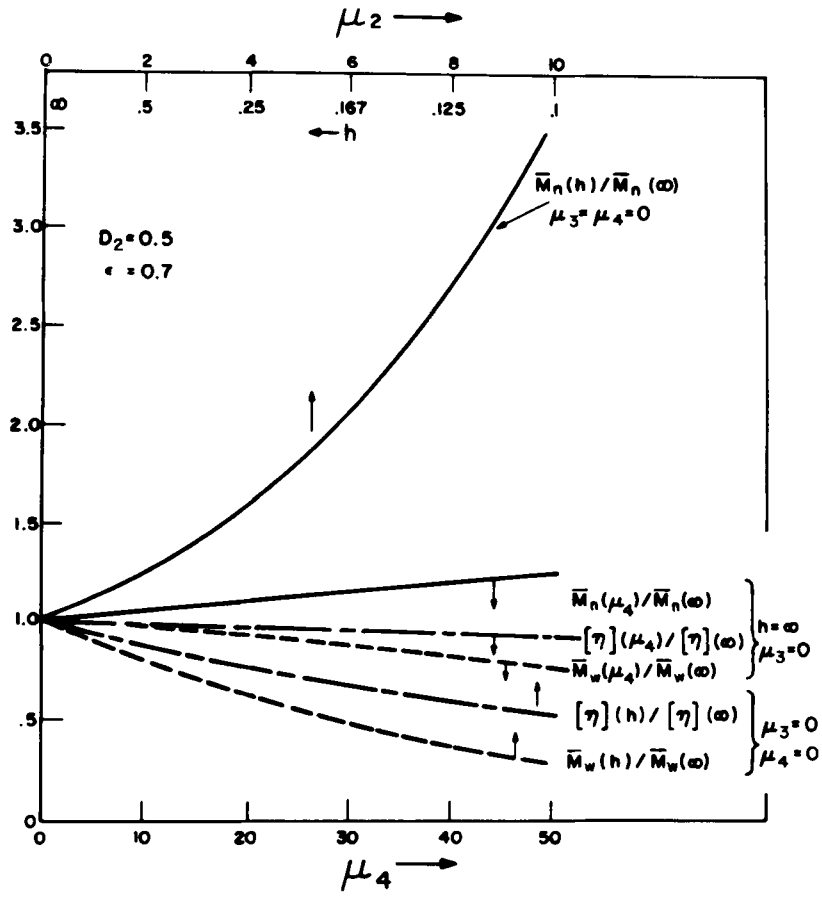

FIG. 5. Correction factor curves for $\bar{M}_n$, $\bar{M}_w$, and $[\eta]$ vs h and μ_2 for $\mu_3 = \mu_4 = 0$ and vs μ_4 for $h = \infty$ and $\mu_3 = 0$.

standards in a symmetric manner in molecular weight space. The exponential term containing h in Eqs. (28), (29), and (30) will serve to enhance the effect of μ_3 on $\bar{M}_n(\infty)$ by dilating the $\bar{M}_n(t)/\bar{M}_n(\infty)$ correction factor and will serve to reduce the effect of μ_3 on $\bar{M}_w(\infty)$ by contracting the $\bar{M}_w(t)/\bar{M}_w(\infty)$ correction factor.

The coefficient μ_4 effects $\bar{M}_n(\infty)$, $\bar{M}_w(\infty)$, and $[\eta](\infty)$ in the same way as does the resolution factor h. For $\mu_4 < 10$ and $D_2 = 0.5$, $\bar{M}_n(\infty)$ is raised and $\bar{M}_w(\infty)$ is lowered by the same amount. The effect of the interaction of μ_4 with μ_3 in Eqs. (43), (44), and (45) is to increase the correction factor for $\bar{M}_n(\infty)$ when $\mu_3 < 0$, and to raise the minimum in

the $\bar{M}_n(\mu_3, \mu_4)/\bar{M}_n(\infty)$ curve when $\mu_3 < 0$. The interaction effect of μ_4 with μ_3 upon $\bar{M}_w(\infty)$ when $\mu_3 < 0$ is to decrease the correction factor for $\bar{M}_w(\infty)$, and when $\mu_3 > 0$ to initially increase the correction factor for $\bar{M}_w(\infty)$ and then decrease it by lowering the maximum in the $\bar{M}_w(\mu_3,\mu_4)/\bar{M}_n(\infty)$ curve. The effect of the interaction of μ_4 with μ_3 on $[\eta](\infty)$ is similar to the effect upon $\bar{M}_w(\infty)$ except that the ϵ-parameter damps out the effect of the quadratic term in μ_3 over the range of μ_3 which is of practical interest.

RESULTS

The values of the absolute and infinite resolution number- and weight-average molecular weights and intrinsic viscosities shown in Table 1 were used in conjunction with Eqs. (28), (29), and (30) to generate values of h, μ_3, and μ_4 which are shown in Tables 3 and 4. These parameters were obtained, with the aid of a CDC-6400 computer,* by a least squares method for estimating nonlinear parameters (*25*) which utilizes a combination of gradient and Newton-Raphson methods. Values of h and μ_3 were obtained by fitting to Eqs. (28) and (29) with $\mu_4 = 0$ ($\{\bar{M}_n, \bar{M}_w\}$ supplied), and fitting to Eqs. (28) and (30) with $\mu_4 = 0$ ($\{\bar{M}_n, [\eta]\}$ supplied). Where the Mark-Houwink coefficients were available, values of h, μ_3, and μ_4 were obtained by fitting to Eqs. (28), (29), and (30) ($\{\bar{M}_n, \bar{M}_w, [\eta]\}$ supplied).

The correlations obtained between μ_3 and PEV for PS, PBD, and PVC standards at a flow rate of 1 ml/min are shown in Fig. 9. The values of μ_3 obtained for each standard by fitting to the parameter sets $\{\bar{M}_n, \bar{M}_w\}$, $\{\bar{M}_n, [\eta]\}$ and $\{\bar{M}_n, \bar{M}_w, [\eta]\}$ agree well within the experimental errors associated with absolute and infinite resolution values of $\bar{M}_n$, $\bar{M}_w$, and $[\eta]$. In fact the values of μ_3 for the polystyrene standards obtained by fitting to $\{\bar{M}_n, \bar{M}_w, [\eta]\}$ are not shown in Fig. 9 because these values would be indistinguishable from the μ_3-values obtained by fitting to $\{\bar{M}_n, \bar{M}_w\}$. The differences in μ_3-values for PS, PVC, and PBD standards over comparable elution volume ranges are very slight. It is interesting to note that the ultranarrow recycle-PS-standards [$P(t) < 1.009$] have slightly lower values of μ_3 (dotted curve) than the narrow PS standards [$1.05 \leq P(t) \leq 1.25$]. The linear portion of the μ_3 vs PEV curve for PS corresponds to the PEV range of optimum

* A Fortran IV computer program which makes use of Marquardt's algorithm to solve a set of nonlinear equations can be found in E. J. Henley and E. M. Rosen, *Material and Energy Balance Computations*, Wiley, New York, 1969, pp. 547f and 560–566.

TABLE 3

Values of h, μ_3, and μ_4 for Polystyrene Standards

Run	PEV	D_2	Fit to $\bar{M}_n$ and $\bar{M}_w$		Fit to $\bar{M}_n$ and $[\eta]$		Fit to $\bar{M}_n$, $\bar{M}_w$, and $[\eta]$		
			h	μ_3	h	μ_3	h	μ_3	μ_4
				Flow Rate = 1 ml/min					
180-176	38.20	0.4896	1.95	−2.53	—	—	—	—	—
180-177	37.60	0.4896	1.88	−1.76	—	—	—	—	—
180-178	36.60	0.4896	2.69	3.06	2.28	2.62	1.67	2.97	0
180-179	34.55	0.4896	1.51	7.17	2.35	8.85	∞	7.78	29.6
180-180	33.25	0.4896	1.49	6.76	3.58	9.56	∞	7.50	29.7
180-182	29.70	0.4580	2.88	7.76	∞	10.7	∞	8.42	13.1
181-183	28.50	0.4580	1.95	7.38	4.69	9.60	∞	7.91	25.0
181-184	28.30	0.4580	1.22	5.56	1.57	6.86	4.23	5.91	32.1
181-185	27.85	0.4580	0.895	1.26	0.957	17.5	1.15	1.29	16.4
181-186	26.25	0.4580	0.531	11.7	0.706	15.4	2.28	13.6	76.8
181-187	25.60	0.4580	1.06	3.21	0.632	−1.03	0.346	2.62	0
181-188	24.60	0.4580	0.631	12.6	0.768	14.8	1.285	13.6	37.0
181-189	23.70	0.4580	0.241	37.8	0.475	61.8	∞	58.7	55.2
181-190	23.65	0.4580	0.213	42.1	0.439	72.2	∞	69.2	11.2
184-207	34.50	0.4896	1.61	3.18	1.74	3.49	2.09	3.23	8.24

184-208	33.45	0.4896	2.39	5.84	71.1	8.80	∞	6.36	20.1
184-209	31.39	0.4580	2.33	4.06	8.08	6.22	∞	4.41	22.7
184-210	29.65	0.4580	2.83	5.09	∞	7.93	∞	5.74	13.0
184-211	28.50	0.4580	1.68	4.76	3.32	6.77	∞	5.21	28.2
184-212	34.51	0.4896	1.59	2.52	1.59	2.52	1.58	2.52	0.390
184-213	33.48	0.4896	2.32	7.86	∞	11.3	∞	8.60	17.9
184-214	31.42	0.4580	2.58	3.97	12.4	6.13	∞	4.31	20.2
				Flow Rate = 2 ml/min					
193-280	37.00	0.4859	1.79	−3.84	1.01	−6.25	0.506	−3.25	0
193-281	35.90	0.4859	2.20	1.52	1.55	3.09	0.925	1.41	0
193-282	33.90	0.4859	1.30	5.92	1.59	6.88	2.94	6.23	1.96
193-283	32.45	0.4409	1.77	3.11	1.93	3.44	1.76	3.10	0.0838
193-285	28.95	0.4409	2.39	1.56	1.93	0.863	1.33	1.51	0
194-286	27.80	0.4409	6.88	5.61	∞	6.81	∞	5.85	5.83
194-287	27.40	0.4409	2.52	−2.80	1.50	−4.55	0.767	−2.57	0
194-288	27.25	0.4409	0.767	−2.39	0.640	−4.06	0.462	−2.20	0
194-289	25.40	0.4409	0.851	2.83	0.774	2.00	0.640	2.73	0
194-290	24.60	0.4409	1.70	−4.67	0.535	−1.23	0.428	−4.49	0
194-291	23.80	0.4409	∞	−3.78	11.3	−7.08	0.818	−3.35	0
194-292	23.10	0.4409	0.413	36.81	1.80	58.0	∞	47.6	16.3
194-293	23.00	0.4409	0.459	39.13	8.28	63.3	∞	49.7	0

TABLE 4

Values of h, μ_3, and μ_4 for Polybutadiene and Polyvinyl Chloride Standards

			Fit to $\bar{M}_n$ and $\bar{M}_w$		Fit to $\bar{M}_n$ and $[\eta]$		Fit to $\bar{M}_n$, $\bar{M}_w$ and $[\eta]$		
Run	PEV	D_2	h	μ_3	h	μ_3	h	μ_3	μ_4
			Polybutadiene, 1 ml/min						
159-045	32.01	0.4785	0.654	5.17	—	—	—	—	—
159-046	27.16	0.4785	0.637	14.6	—	—	—	—	—
159-047	26.10	0.4785	0.485	6.61	—	—	—	—	—
159-048	25.80	0.4785	0.303	9.38	—	—	—	—	—
159-049	25.22	0.5693	0.302	10.5	—	—	—	—	—
			Polyvinyl Chloride, 1 ml/min						
158-042	30.80	0.4750	∞	5.35	1.52	−0.653	0.339	3.83	0
158-043	29.70	0.4750	∞	6.98	∞	3.97	1.52	6.48	0
158-044	29.31	0.4750	5.51	8.49	2.53	6.95	0.969	7.71	0

resolution in the molecular weight calibration curve. The upturn at low PEV (high molecular weight) to large μ_3-values and the downturn at high PEV (low molecular weight) to negative μ_3-values is due to the loss of resolution at the high and low molecular weight ends of the calibration curve. The increase in μ_3 to large positive values can be expected to be greater than the decrease in μ_3 to large negative values because of increased viscosity effects at the high molecular weight end of the calibration curve.

The correlations obtained between h and PEV for PS and PBD standards at a flow rate of 1 ml/min by fitting to the parameter sets $\{\bar{M}_n, \bar{M}_w\}$ and $\{\bar{M}_n, [\eta]\}$ are shown in Figs. 6 and 8. A scatter envelope (dotted curves) corresponding to reasonable experimental errors is shown in Fig. 6 for the polystyrene standards. The observed scatter in the data can be attributed to uncertainties in the experimental number- and weight-average molecular weights (particularly at low molecular weights), and the Mark-Houwink coefficients of the narrow MWD standards.

The recycle-PS-standards scatter to the same extent as the broader PS standards. The values of h obtained for the PVC standards were extremely scattered. The experimental polydispersity of these samples was greater than the GPC infinite resolution values and was reproducible. This can be attributed to possible experimental errors in the determination of $\bar{M}_n(t)$ and $\bar{M}_w(t)$, and the nature of the molecular weight

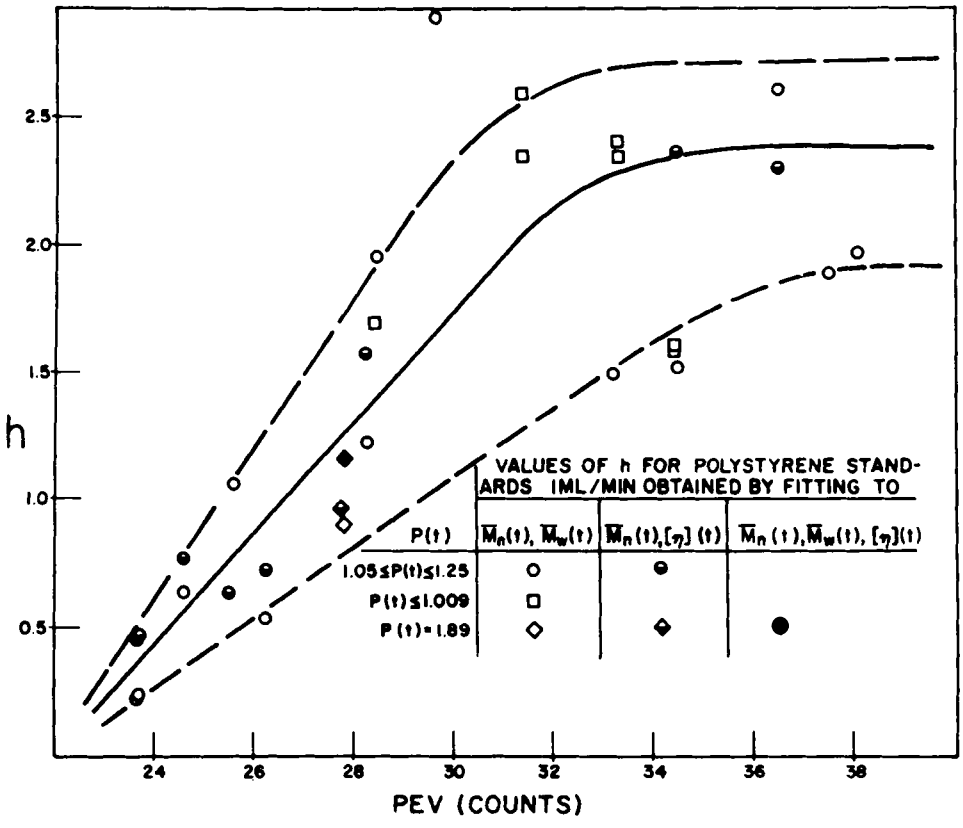

FIG. 6. Resolution factor h vs PEV for polystyrene, 1 ml/min flow rate.

calibration curve. At first the weight-average and viscosity-average molecular weights were associated with PEV to obtain a calibration curve. This resulted in $\bar{M}_w(\infty) > \bar{M}_w(t)$, $\bar{M}_n(\infty) > \bar{M}_n(t)$, and $P(\infty) < P(t)$. Then, $[\bar{M}_n(t) \cdot \bar{M}_w(t)]^{1/2}$ was associated with PEV. This resulted in the more usual GPC conditions, $\bar{M}_n(\infty) < \bar{M}_n(t)$ and $\bar{M}_w(\infty) \leq \bar{M}_w(t)$. However, $P(\infty) < P(t)$. This condition could result from the limited elution volume-molecular weight range obtained from experiment and the necessary extrapolation of the molecular weight calibration curve outside this range for the calculation of $\bar{M}_n(\infty)$, $\bar{M}_w(\infty)$, and $[\eta](\infty)$. However, a rather large increase in the slope of the calibration curve ($D_2/2.303$) would be necessary for $P(\infty) \geq P(t)$. Meyerhoff (*26*) also has observed this phenomena with broad standards. He attributes

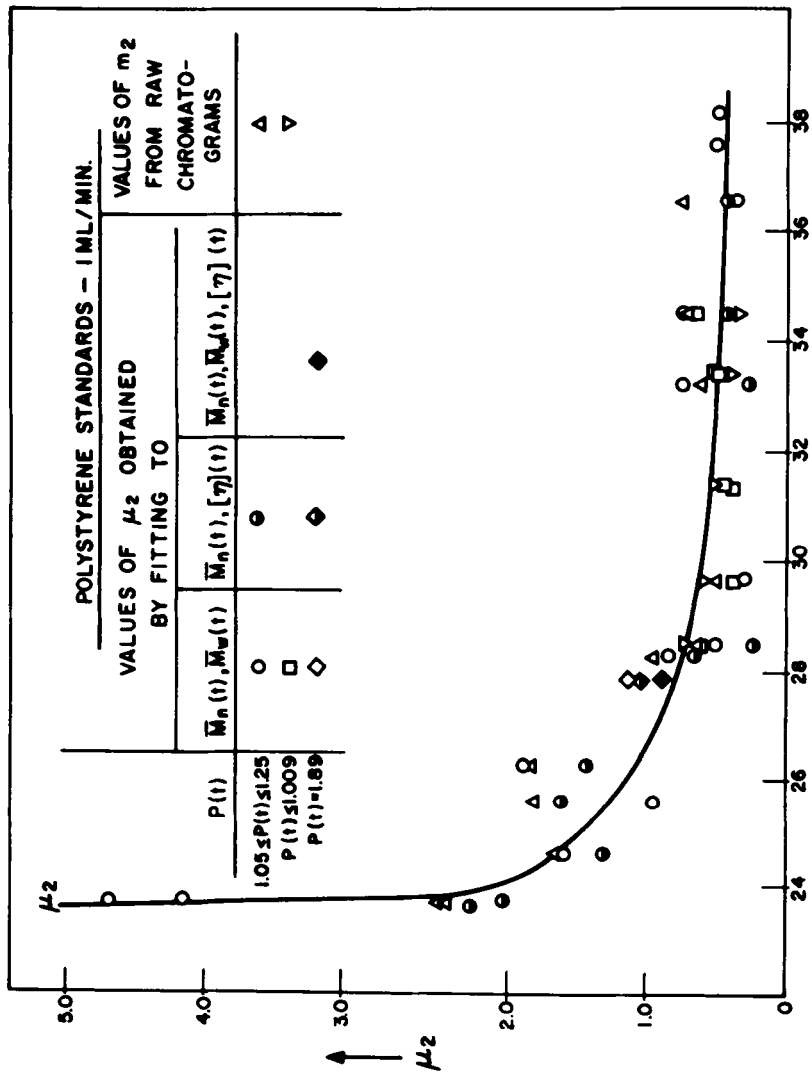

FIG. 7. Variance μ_2 vs PEV for polystyrene, 1 ml/min flow rate.

this behavior to extremely high resolving power of GPC columns over the elution volume range of the samples.

Since the magnitude of the correction for axial dispersion is inversely proportional to h, it is more useful to look at a plot of μ_2 vs PEV when assessing the effects of experimental scatter in h on the magnitude of the correction. Such a plot for PS standards at a flow rate of 1 ml/min is shown in Fig. 7. For typical experimental uncertainty ranges in h of $1.4 \leq h \leq 2.8$, $0.8 \leq h \leq 1.6$, and $0.28 \leq h \leq 0.6$ (corresponding to ranges in μ_2 of $0.36 \leq \mu_2 \leq 0.71$, $0.63 \leq \mu_2 \leq 1.25$, and $1.7 \leq \mu_2 \leq 3.6$), the corresponding ranges in the correction factors obtainable from Fig. 3 are, respectively: $1.06 \leq \bar{M}_n(t)/\bar{M}_n(\infty)$, $\bar{M}_w(t)/\bar{M}_w(\infty) \leq 1.10$; $1.09 \leq \bar{M}_n(t)/\bar{M}_n(\infty), \bar{M}_w(t)/\bar{M}_w(\infty) \leq 1.16$; and $1.22 \leq \bar{M}_w(t)/\bar{M}_w(\infty) \leq 1.56$, $1.16 \leq \bar{M}_n(t)/\bar{M}_n(\infty) \leq 1.37$. For $h > 0.6$, the magnitude of the errors in the correction factors produced by the experimental uncertainties in h are not too severe and can be tolerated.

A similar analysis of the effect of experimental errors in μ_3 upon the correction factors obtainable from Fig. 4 can be done. For $6 \leq \mu_3 \leq 12$, the range in the correction factor is $1.12 \leq \bar{M}_n(t)/\bar{M}_n(\infty), \bar{M}_n(t)/\bar{M}_w(\infty) \leq 1.26$. For $25 \leq \mu_3 \leq 40$, the range in correction factors is $1.64 \leq \bar{M}_n(t)/\bar{M}_n(\infty) \leq 2.18$ and $1.8 \leq \bar{M}_w(t)/\bar{M}_w(\infty) \leq 1.96$. Thus at large values of μ_3, where loss of resolution in the calibration curve is observed, extreme errors in the correction factors are obtained.

When values of h, μ_3, and μ_4 at a flow rate of 1 ml/min are obtained by fitting to the parameter set $\{\bar{M}_n, \bar{M}_w, [\eta]\}$, the values of h are generally much larger than those obtained by fitting to the parameter sets $\{\bar{M}_n, \bar{M}_w\}$ or $\{\bar{M}_n, [\eta]\}$. In fact, for most cases, h is sufficiently large that the exponential factors $\exp(\pm D_2^2/2h) \simeq 1$ and the correction equations in μ_3 and μ_4 (Eqs. 43, 44, and 45) can be used to compute the corrected values $\bar{M}_n(\mu_3,\mu_4)$, $\bar{M}_w(\mu_3,\mu_4)$ and $[\eta](\mu_3,\mu_4)$. Both h and μ_4 are measures of dispersion in elution volume space and thus interact. The large values of h (small values of μ_2) obtained in this manner indicate that at a flow rate of 1 ml/min the parameter of μ_4 is a stronger function of the dispersion than is h. A plot of μ_4 vs PEV is shown in Fig. 10.

Earlier in this paper it was pointed out that the computed second, third, and fourth moments, m_2, m_3, and m_4, about the mean elution volume of the normalized observed chromatogram would be equivalent to the moments μ_2, μ_3, and μ_4 of the general shape function in the limit of the ideal monodisperse standard, $P(t) = 1$. The computed moments m_2, m_3, and m_4 of some of the polystyrene standards at 1 ml/min. flow rate are shown in Table 5. Values of m_2 are directly compared with μ_2 in

TABLE 5

Values of m_2, m_3, and m_4 for Polystyrene Standards, 1 ml/min Obtained from the Normalized Observed Chromatograms

Run	m_2	m_3	m_4
180-178	0.767	0.276	18.6
180-179	0.663	0.284	17.0
180-180	0.600	0.135	12.1
180-182	0.540	0.335	13.9
181-183	0.642	0.473	21.2
181-184	0.933	0.457	42.2
181-185	4.04	3.49	51.2
181-186	1.83	3.39	19.1
181-187	1.80	3.17	17.4
181-188	1.69	3.46	17.3
181-189	2.49	5.83	33.0
181-190	2.46	5.69	31.6
184-207	0.318	0.0471	0.317
184-208	0.406	0.128	0.572
184-209	0.524	0.450	1.60
184-210	0.556	0.350	1.27
184-211	0.650	0.479	1.93

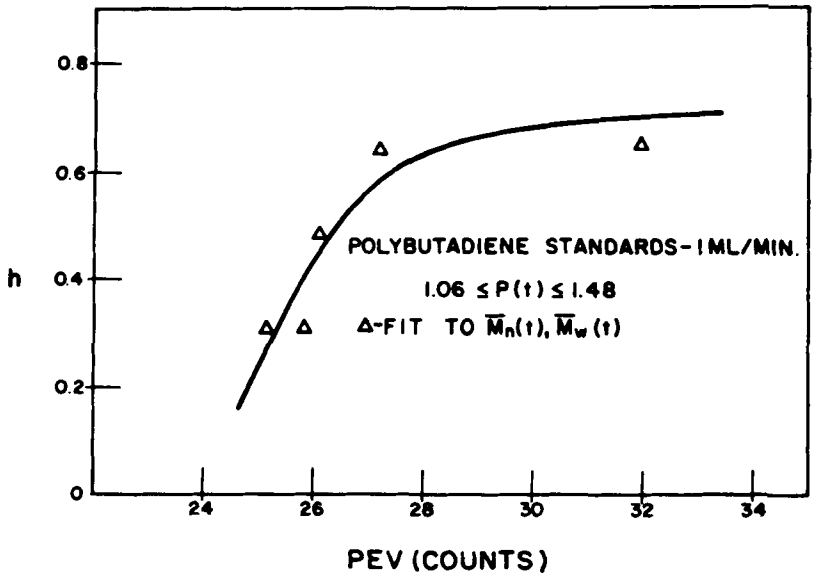

FIG. 8. Resolution factor h vs PEV for polybutadiene, 1 ml/min flow rate.

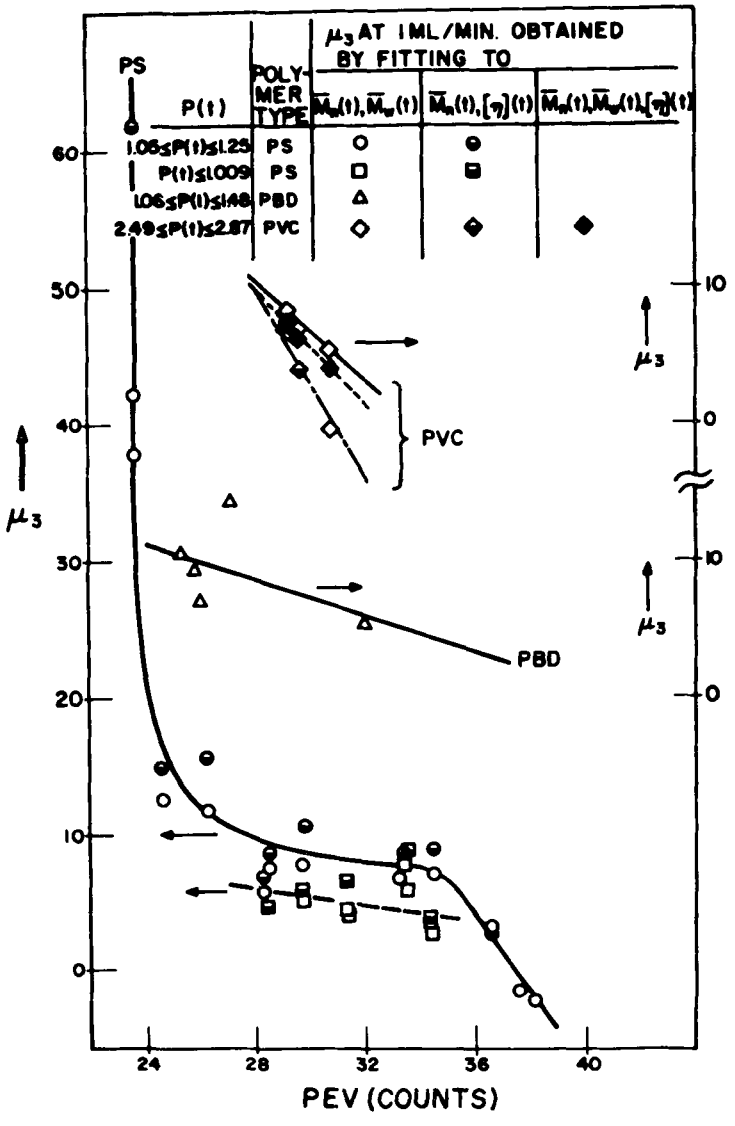

FIG. 9. Skewing coefficient μ_3 vs PEV for polystyrene, polybutadiene, and polyvinyl chloride, 1 ml/min flow rate.

Fig. 5. In general $\mu_2 \approx m_2$ for these standards. Comparison of m_3 in Table 5 with μ_3 in Table 3 shows that $\mu_3 \gg m_3$. Similarly $\mu_4 > m_4$ as shown in Fig. 8. The large differences between m_3 and μ_3 and m_4 and μ_4 are attributable to the natural skewness and flatness associated with

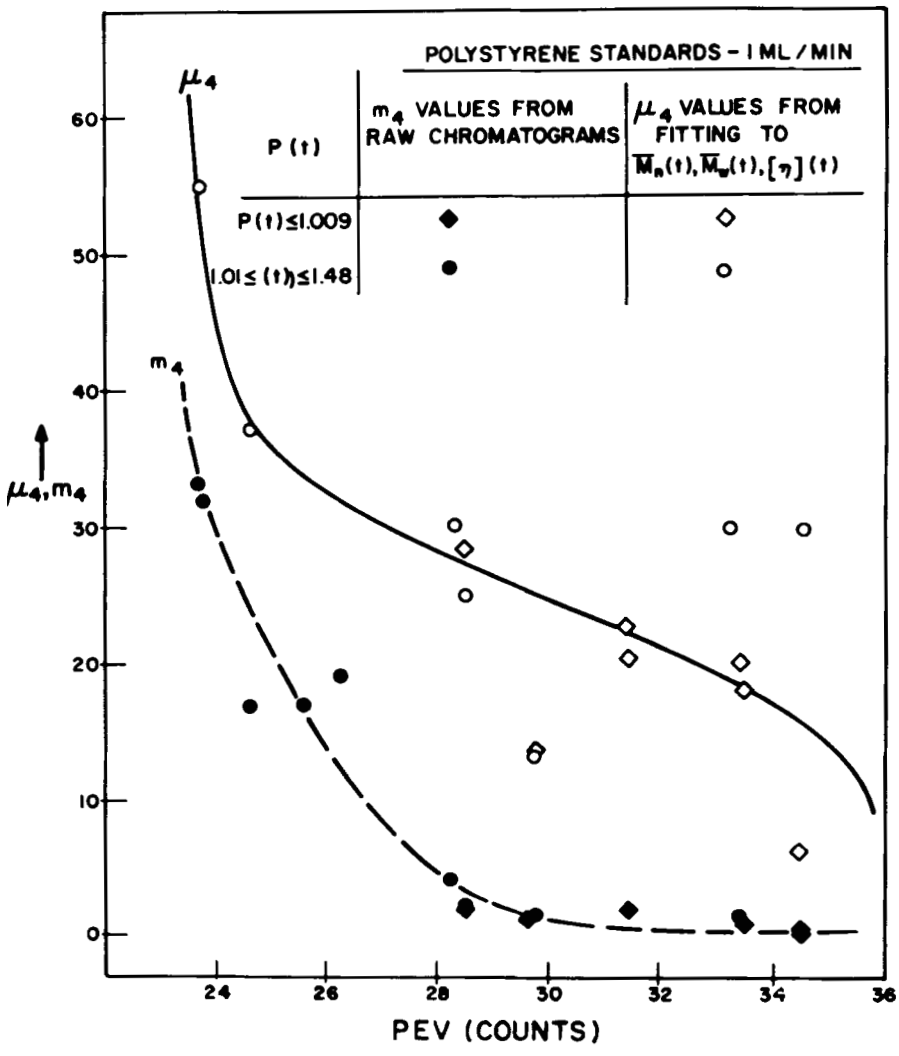

FIG. 10. μ_4, m_4 vs PEV for polystyrene, 1 ml/min flow rate.

the MWD of the PS-calibration standards, the approximation of the molecular weight calibration curve by two linear segments, and the experimental errors associated with determination of $\bar{M}_n(t)$, $\bar{M}_w(t)$, and $[\eta](t)$.

$\bar{M}_n(\infty)$, $\bar{M}_w(\infty)$, and $[\eta](\infty)$ (where applicable) for PS and PBD-

TABLE 6

Corrected Values of $\bar{M}_n$, $\bar{M}_w$, and $[\eta]$ for Polystyrene Standards, 1 ml/min

Run	$10^{-3}\bar{M}_n(h,\mu_3)$	$10^{-3}\bar{M}_w(h,\mu_3)$	$[\eta](h,\mu_3)$	$P(h,\mu_3)$	$10^{-3}\bar{M}_n(\mu_3,\mu_4)$	$10^{-3}\bar{M}_w(\mu_3,\mu_4)$	$[\eta](\mu_3,\mu_4)$	$P(\mu_3,\mu_4)$
180-176	1.20	1.42	—	1.18	—	—	—	—
180-177	1.75	1.92	—	1.10	—	—	—	—
180-178	3.16	3.46	0.0492	1.10	3.04	3.60	0.0503	1.18
180-179	9.44	10.6	0.106	1.12	9.35	10.6	0.107	1.13
180-180	19.4	20.8	0.167	1.07	19.3	20.6	0.170	1.07
180-182	103	100	0.504	<1.0	103	98.8	0.514	<1.0
181-183	172	175	0.759	1.02	168	176	0.777	1.05
181-184	178	193	0.808	1.08	174	195	0.829	1.12
181-185	149	309	1.067	2.07	145	312	1.095	2.15
181-186	360	446	1.433	1.23	342	457	1.489	1.34
181-187	482	588	1.731	1.22	450	609	1.815	1.35
181-188	834	928	2.351	1.11	748	980	2.522	1.31
181-189	1420	2176	3.231	1.53	1229	1714	3.554	1.39
181-190	1480	2573	3.303	1.73	1303	1738	3.600	1.33
184-207	10.0	10.4	0.108	1.04	9.90	10.5	0.110	1.06
184-208	16.3	16.2	0.145	~1.0	16.2	16.2	0.147	1.00
184-209	43.0	42.9	0.288	~1.0	42.5	43.2	0.292	1.02
184-210	97.2	92.2	0.493	<1.0	95.7	92.6	0.503	<1.0
184-211	161	162	0.736	1.006	157	165	0.754	1.05
184-212	10.1	10.6	0.109	1.05	9.99	10.6	0.111	1.06
184-213	15.9	15.7	0.142	~1.0	15.8	15.7	0.144	~1.0
184-214	43.2	42.8	0.288	~1.0	42.7	43.0	0.292	1.007

TABLE 7

Corrected Values of $\bar{M}_n$ and $\bar{M}_w$ for Polybutadiene Standards, 1 ml/min

Run	$10^{-3}\bar{M}_n(h,\mu_3)$	$10^{-3}\bar{M}_w(h,\mu_3)$	$P(h,\mu_3)$
159-045	16.2	17.5	1.08
159-046	126	147	1.17
159-047	221	287	1.30
159-048	208	307	1.78
159-049	288	426	1.48

calibration standards at a flow rate of 1 ml/min have been corrected for skewing and axial dispersion with the aid of Eqs. (28), (29), and (30) using values of h, μ_3, and μ_4 obtained from the average smooth curves drawn in Figs. 6, 8, 9, and 10. The corrected data is shown in Tables 6 and 7. $\bar{M}_n(\mu_3,\mu_4)$, $\bar{M}_w(\mu_3,\mu_4)$, and $[\eta](\mu_3,\mu_4)$ have been calculated from Eqs. (43), (44), and (45) under the assumption that h is very large ($\mu_2 \simeq 0$). There is good agreement between the corrected values $\bar{M}_n(\mu_3,\mu_4)$, $\bar{M}_w(\mu_3,\mu_4)$, and $[\eta](\mu_3,\mu_4)$ and the corrected values $\bar{M}_n(h,\mu_3)$, $\bar{M}_w(h,\mu_3)$, and $[\eta](h,\mu_3)$ when the h referred to in the data set $\{h,\mu_3,\mu_4\}$ of Table 3 is greater than 2. Also, the corrected value of $\bar{M}_n$, $\bar{M}_w$, and $[\eta]$ compare favorably with the true values, $\bar{M}_n(t)$, $\bar{M}_w(t)$, and $[\eta](t)$ of Table 1. Most of the corrected values lie well within the range of the experimental errors associated with the determination of $\bar{M}_n(t)$, $\bar{M}_w(t)$, $[\eta](t)$, and $P(t)$. Deviations occur for the very broad standard NBS-706, and for the ultrahigh molecular weight standards ($M \geq 10^6$) where the uncertainties in h, μ_3, and μ_4 are very large.

The PS-calibration standards run at 2 ml/min yielded values of h slightly smaller than those at 1 ml/min, while the values of μ_3 and μ_4 at 2 ml/min were considerably smaller than those at 1 ml/min. The values of μ_3 at 2 ml/min scattered considerably more than at 1 ml/min. This scatter can be attributed to baseline instabilities at the higher flow rate and a smaller data sampling frequency. Values of h and μ_3 at 1 ml/min obtained by fitting to the parameter sets $\{\bar{M}_n, \bar{M}_w\}$ and $\{\bar{M}_n, [\eta]\}$, and values of h, μ_3, and μ_4 at 2 ml/min obtained by fitting to the parameter set $\{\bar{M}_n, \bar{M}_w, [\eta]\}$ are shown in Table 3. When the flow rate is increased from 1 to 2 ml/min, there is an increase in instrument spreading due to axial dispersion and a reduction in instrument spreading due to skewing and flattening.

Some polystyrene blends run at a flow rate of 2 ml/min having complex multimodal shapes shown in Figs. 2 and 3, and having a poly-

TABLE 8

Corrected Values of $\bar{M}_n$, $\bar{M}_w$, $[\eta]$, and P for Polystyrene Blends, 2 ml/min for Ranges of h and μ_3 Values

Run	h	μ_3	$10^{-3}\bar{M}_n(h,\mu_3)$	$10^{-3}\bar{M}_w(h,\mu_3)$	$[\eta](h,\mu_3)$	$P(h,\mu_3)$
196-302-2	1.7	1.5	66.9	71.3	0.419	1.06
	1.7	3.0	68.3	72.7	0.422	1.06
	2.4	1.5	65.8	72.3	0.423	1.10
	2.4	3.0	67.2	74.0	0.426	1.10
196-303-2	1.7	1.5	29.1	35.5	0.253	1.22
	1.7	3.0	29.7	36.3	0.255	1.22
	2.4	1.5	28.6	36.1	0.255	1.26
	2.4	3.0	29.2	36.9	0.257	1.26
196-304-2	1.7	1.5	33.1	59.7	0.356	1.80
	1.7	3.0	33.7	61.0	0.358	1.81
	2.4	1.5	32.6	60.6	0.358	1.86
	2.4	3.0	33.2	62.0	0.361	1.86
196-305-2	1.7	1.5	23.6	28.2	0.215	1.20
	1.7	3.0	24.1	28.8	0.216	1.20
	2.4	1.5	23.2	28.7	0.216	1.24
	2.4	3.0	23.7	29.3	0.218	1.24
196-306-2	1.7	1.5	37.1	41.1	0.283	1.11
	1.7	3.0	37.9	42.0	0.285	1.11
	2.4	1.5	36.5	41.8	0.286	1.15
	2.4	3.0	37.2	42.7	0.288	1.15
196-307-2	1.7	1.5	37.4	54.9	0.340	1.47
	1.7	3.0	38.2	56.1	0.342	1.48
	2.4	1.5	36.8	55.8	0.343	1.52
	2.4	3.0	37.6	57.1	0.345	1.52
196-308-2	1.7	1.5	50.9	68.0	0.401	1.34
	1.7	3.0	52.0	69.6	0.404	1.34
	2.4	1.5	50.1	69.2	0.404	1.38
	2.4	3.0	51.1	70.7	0.407	1.38
196-309-2	1.7	1.5	30.1	42.9	0.284	1.43
	1.7	3.0	30.7	43.8	0.286	1.43
	2.4	1.5	29.6	43.6	0.287	1.47
	2.4	3.0	30.2	44.5	0.289	1.48

dispersity range $1.11 \leq P(t) \leq 1.79$, were corrected for axial dispersion and skewing. Values of h and μ_3, obtained from calibration standards covering the elution volume range of these blends, were in the ranges $1.7 \leq h \leq 2.4$ and $1.5 \leq \mu_3 \leq 3.0$, respectively. Corrected values of $\bar{M}_n(h,\mu_3)$, $\bar{M}_w(h,\mu_3)$, $[\eta](h,\mu_3)$, and $P(h,\mu_3)$ are shown in Table 8 for $h = 1.7$ and 2.4, and $\mu_3 = 1.5$ and 3.0. These corrected values compare

favorably with the absolute values in Table 2 over a reasonably wide range of experimental uncertainties in h and μ_3 values.

More experimental work is needed to ascertain whether broad calibration standards, $P(t) > 2$, can be used to obtain valid values of h, μ_3, and μ_4. The main problem with using broad MWD standards is that average values of h, μ_3, and μ_4 will be obtained over wide elution volume ranges. These values will be unreliable if h, μ_3, and μ_4 are changing rapidly over the elution volume range. For these reasons, values of h, μ_3, and μ_4 obtained from narrow MWD standards may tend to overcorrect very broad MWD standards. A method will be proposed in the next section that will circumvent this problem.

CORRECTION METHODS FOR THE DMWD CURVE

Fitting for an Effective Linear Calibration

If the calibration curve is truly linear over the molecular weight range of interest, the corrected values $\bar{M}_n(t)$ and $\bar{M}_w(t)$ can be used to fit for the slope and intercept of the corrected calibration curve. Then, the corrected DMWD curve can be obtained from this corrected calibration curve. Hamielec and co-workers (*11*, *27*) have demonstrated the feasibility of this approach. If the corrected molecular weight calibration constants are denoted by $D_1(t)$ and $D_2(t)$, and the infinite resolution values by $D_1(\infty)$ and $D_2(\infty)$, then

$$\frac{\bar{M}_n(t)}{\bar{M}_n(\infty)} = \left(\frac{D_1(t)}{D_1(\infty)}\right)\frac{\bar{F}[-D_2(\infty)]}{\bar{F}[-D_2(t)]} \tag{48}$$

$$\frac{\bar{M}_w(t)}{\bar{M}_w(\infty)} = \left(\frac{D_1(t)}{D_1(\infty)}\right)\frac{\bar{F}[D_2(t)]}{\bar{F}[D_2(\infty)]} \tag{49}$$

Use of Eqs. (48) and (49) with (36) and (37) yields the following useful relations

$$\frac{\bar{F}[-D_2(\infty)]\bar{F}[D_2(\infty)]}{\bar{F}[-D_2(t)]\bar{F}[D_2(t)]} = \exp\left[D_2^2(\infty)/h\right]\{1 - [D_2^3(\infty)\mu_3/6]^2\} \tag{50}$$

$$D_1(t) = D_1(\infty)\left\{\left(\frac{1 + D_2^3(\infty)\mu_3/6}{1 - D_2^3(\infty)\mu_3/6}\right)\left(\frac{\bar{F}[-D_2(t)]\bar{F}[D_2(\infty)]}{\bar{F}[-D_2(\infty)]\bar{F}[D_2(t)]}\right)\right\}^{1/2} \tag{51}$$

where $\bar{F}$ is the previously defined bilateral Laplace transform function. Equation (50) shows that the slope of the corrected calibration curve $[D_2(t)/2.303]$ is a function of $D_2(\infty)$, h, and μ_3. Equation (51) shows that the intercept of the corrected calibration curve $[\log_{10} D_1(t)]$ is a function

of $D_1(\infty)$, $D_2(\infty)$, h, and μ_3. Thus, in order to compensate for the effects of skewing and axial dispersion, the calibration curve must be both translated and rotated.

The Hydrodynamic Volume Concept Approach

Another method which is useful for correcting the infinite resolution DMWD for skewing and axial dispersion involves the use of the hydrodynamic volume concept. Benoit et al. (*28*) have shown that when the product $\{[\eta]\bar{M}_w\}$ is plotted against PEV, a common calibration curve results for linear and branched homopolymers and grafted copolymers. In particular, they have shown that linear PS, PBD, and PVC fall on a common $\{[\eta]\bar{M}_w\}$ vs PEV plot. Pickett et al. (*14*) have obtained expressions for $\bar{M}_n$ and $\bar{M}_w$ in terms of the DMWD, (da/dM), as follows:

$$\bar{M}_n = \left[\int_{M_L}^{M_H} \frac{1}{M}\left(\frac{da}{dM}\right) dM\right]^{-1} \tag{52}$$

$$\bar{M}_w = \int_{M_L}^{M_H} M\left(\frac{da}{dM}\right) dM \tag{53}$$

where

$$\frac{da}{dM} = \frac{C(v_M)}{\int_{v_H}^{v_L} C(v)\, dv} \cdot \frac{1}{\left(\frac{df}{dv}\right)_{v_M}} \cdot \frac{\log_{10} e}{M} \tag{54}$$

The first term on the right-hand side of Eq. (54) is the normalized chromatogram height at elution volume v_M and the second term is the reciprocal of the slope of the calibration curve, $f(v) = \log_{10} M$. Expressing the hydrodynamic volume as

$$Z = \{[\eta]M\} = KM^{\epsilon+1} \tag{55}$$

where K and ϵ are the standard Mark-Houwink parameters, and substituting this expression into Eqs. (52), (53), and (54) leads to the expressions

$$\bar{M}_n = \left[\int_{Z_L}^{Z_H} \left(\frac{Z}{K}\right)^{1/(\epsilon+1)} \left(\frac{da}{dZ}\right) dZ\right]^{-1} \tag{56}$$

$$\bar{M}_w = \int_{Z_L}^{Z_H} \left(\frac{Z}{K}\right)^{1/(\epsilon+1)} \left(\frac{da}{dZ}\right) dZ \tag{57}$$

$$\frac{da}{dZ} = \frac{C(v_Z)}{\int_{v_H}^{v_L} C(v)\,dv} \cdot \frac{1}{\left(\frac{df'}{dv}\right)_{v_Z}} \cdot \frac{\log_{10} e}{Z} \tag{58}$$

where now the hydrodynamic volume calibration curve is expressed as $f'(v) = \log_{10} Z$. By using the corrected values of $\bar{M}_n(t)$ and $\bar{M}_w(t)$ obtained from Eqs. (28) and (29) in conjunction with the hydrodynamic volume calibration curve, Eqs. (56) and (57) can be fit for effective values of ϵ and K that correct the infinite resolution values, $\bar{M}_n(\infty)$ and $\bar{M}_w(\infty)$ to the true values $\bar{M}_n(t)$ and $\bar{M}_w(t)$. Once ϵ and K are obtained, the corrected molecular weight calibration curve can be obtained from Eq. (55) and, subsequently, the corrected DMWD can be obtained from Eq. (54). The relationship between the corrected calibration curve, $f_t(v) = \log_{10} M_t$, and the uncorrected curve $f(v)$ can be expressed, according to the formalism of Coll and Prusinowski (*29*), as

$$\log_{10} M_t = \left(\frac{1}{1+\epsilon_t}\right) \log_{10}\left(\frac{K}{K_t}\right) + \left(\frac{1+\epsilon}{1+\epsilon_t}\right) f(v) \tag{59}$$

where ϵ and K are the Mark-Houwink parameters used in the construction of the hydrodynamic volume calibration curve, and ϵ_t and K_t are the effective Mark-Houwink parameters obtained upon fitting Eqs. (56) and (57) to $\bar{M}_n(t)$ and $\bar{M}_w(t)$. This hydrodynamic volume approach for obtaining the corrected DMWD curves is quite general and does not require a linear molecular weight calibration curve over the entire elution volume range of interest. For the special case of a linear calibration curve, the coefficients $D_1(t)$ and $D_2(t)$ of the corrected calibration curve can be related to the coefficients $D_1(\infty)$ and $D_2(\infty)$ of the uncorrected curve with the aid of Eqs. (6) and (59).

$$D_1(t) = \left(\frac{K}{K_t}\right)^{1/(1+\epsilon_t)} (D_1(\infty))^{(1+\epsilon)/(1+\epsilon_t)} \tag{60}$$

$$D_2(t) = \left(\frac{1+\epsilon}{1+\epsilon_t}\right) D_2(\infty) \tag{61}$$

From the previous analysis made with Eqs. (50) and (51), it can be seen that ϵ_t is a function of $D_2(\infty)$, ϵ, h, and μ_3 while K_t is a function of $D_1(\infty)$, ϵ, K, $D_2(\infty)$, h, and μ_3. Thus, both K_t and ϵ_t are affected by GPC chromatogram spreading due to axial dispersion and skewing.

The DMWD curves of several of the standards have been corrected by this hydrodynamic volume fitting procedure. The mathematical method (*25*) used in the fitting procedure has been discussed previously.

TABLE 9

Fitted Values of ϵ_t and K_t and Calculated Values of $\bar{M}_n(t)$, $\bar{M}_w(t)$, $[\eta](t)$, and $P(t)$

Run	ϵ_t	10^3K_t	Calculated values			
			$10^{-3}\bar{M}_n(t)$	$10^{-3}\bar{M}_w(t)$	$[\eta](t)$	$P(t)$
Polyvinyl Chloride, 1 ml/min						
158-042	0.474	2.39	25.5	68.7	0.799	2.70
158-043	0.283	20.6	41.1	118	1.202	2.87
158-044	0.437	3.78	54.9	127	1.253	2.30
Polybutadiene, 1 ml/min						
159-047	0.865	0.0335	200	282	—	1.41
159-049	1.10	0.0010	265	443	—	1.67
Polystyrene, 1 ml/min						
180-177	0.727	0.145	1.69	1.89	—	1.12
180-178	0.548	0.498	3.18	3.53	0.0489	1.11
180-179	0.749	0.0862	9.71	10.3	1.053	1.06
181-185	0.871	0.0188	135	261	0.944	1.94
181-186	0.603	0.337	392	412	1.277	1.05
Polystyrene Blends, 2 ml/min						
196-302-2	0.799	0.0541	64.3	75.4	0.435	1.17
196-303-2	0.865	0.0309	27.7	35.9	0.255	1.30
196-304-2	0.871	0.0269	32.6	59.0	0.355	1.81
196-305-2	0.907	0.0208	22.5	28.3	0.215	1.26
196-306-2	0.782	0.0684	35.5	43.3	0.293	1.22
196-307-2	0.843	0.0352	36.7	56.3	0.346	1.54
196-308-2	0.814	0.0485	48.7	69.6	0.408	1.48
196-309-2	0.872	0.0271	29.4	43.3	0.287	1.47

The hydrodynamic volume calibration curve was obtained from the $[\eta](t)$–$\bar{M}_w(t)$ data for polystyrene in Table 1. The values of $\bar{M}_n(t)$ and $\bar{M}_w(t)$ used in the fitting of Eqs. (56) and (57) are listed in Table 1. The values of ϵ_t and K_t obtained from the fit along with values of $\bar{M}_n(t)$, $\bar{M}_w(t)$, $[\eta](t)$, and $P(t)$ calculated from the fitted ϵ_t and K_t values are shown in Table 9. Some plots of the uncorrected and corrected DMWD curves $[da/dM](\infty)$ and $[da/dM](t)$, respectively, are shown in Figs. 11–16. The values of $\bar{M}_n(t)$, $\bar{M}_w(t)$, $[\eta](t)$, and $P(t)$ in Table 9 are in excellent agreement with the corresponding values in Table 1. The range of values in ϵ_t and K_t shown in Table 9 for PS samples reflect the dispersion and skewing corrections, experimental errors in $\bar{M}_n(t)$ and $\bar{M}_w(t)$, and chromatogram baseline errors.

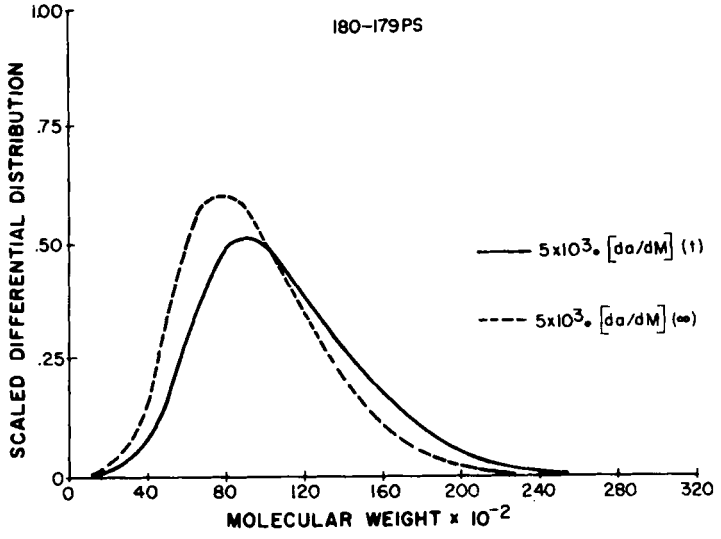

FIG. 11. Corrected and infinite resolution DMWD vs M curves for polystyrene sample 180-179.

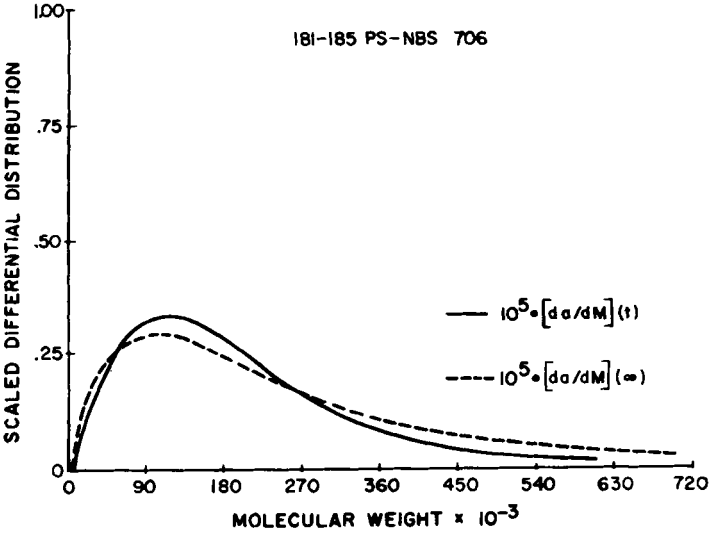

FIG. 12. Corrected and infinite resolution DMWD vs M curves for polystyrene sample 181-185.

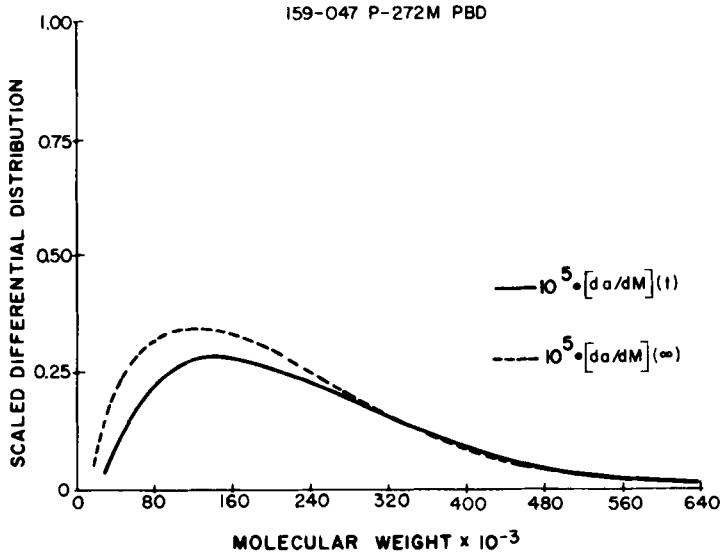

FIG. 13. Corrected and infinite resolution DMWD vs M curves for polybutadiene sample 159-047.

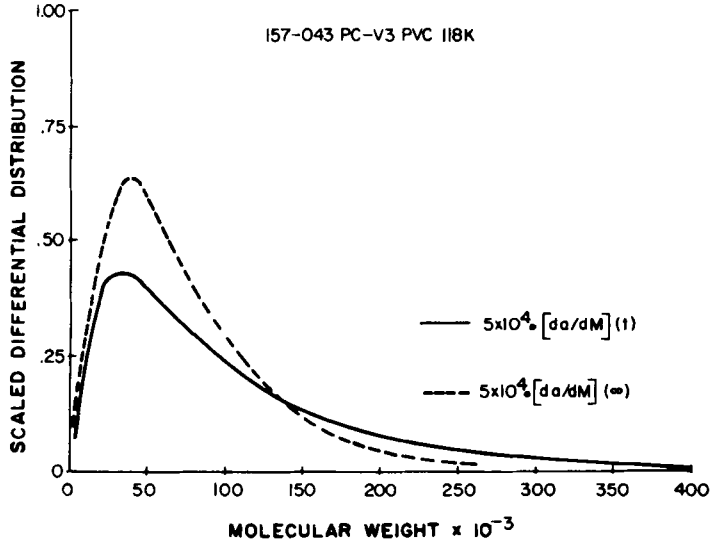

FIG. 14. Corrected and infinite resolution DMWD vs M curves for polyvinyl chloride sample 157-043.

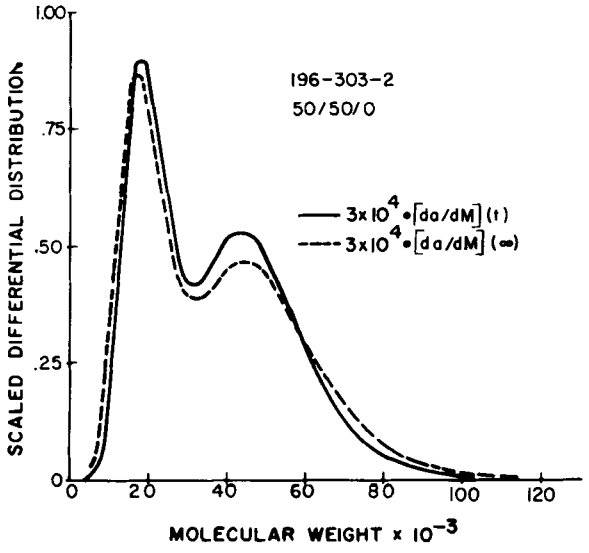

FIG. 15. Corrected and infinite resolution DMWD vs M curves for polystyrene blend 196-303-2.

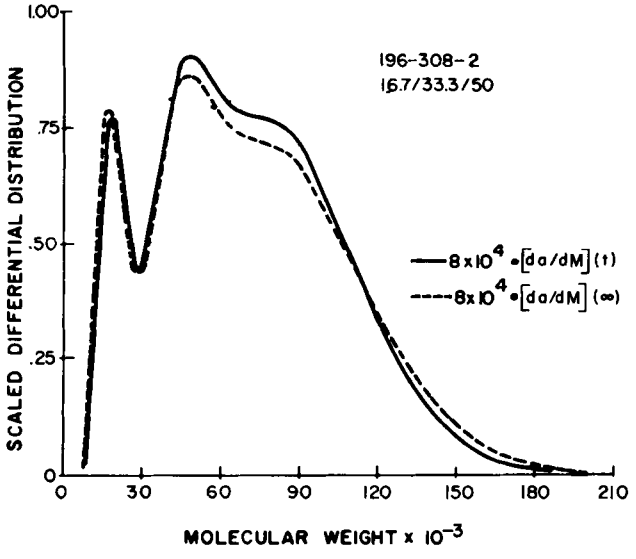

FIG. 16. Corrected and infinite resolution DMWD vs M curves for polystyrene blend 196-308-2.

In principle, the corrected chromatogram $W(v)$ can be obtained from the DMWD curve corrected by the hydrodynamic volume fitting procedure. However, by use of Eq. (54), $W(v)$ can be expressed in terms of $F(v)$ and the uncorrected and corrected molecular weight calibration curves. The corrected DMWD curve obtained from $W(v)$ is given by

$$\left[\frac{da}{dM}\right](t) = W(v) \cdot \frac{1}{\left(\frac{df}{dv}\right)_{v_{M(\infty)}}} \cdot \frac{\log_{10} e}{M(\infty)} \tag{62}$$

and the corrected DMWD curve obtained from the hydrodynamic volume fitting procedure is given by

$$\left[\frac{da}{dM}\right](t) = F(v) \cdot \frac{1}{\left(\frac{df_t}{dv}\right)_{v_{M_t}}} \cdot \frac{\log_{10} e}{M_t} \tag{63}$$

Combining Eqs. (62) and (63) yields

$$W(v) = F(v)\left[\left(\frac{df}{dv}\right)_{v_{M(\infty)}} \Big/ \left(\frac{df_t}{dv}\right)_{v_{M_t}}\right]\left[\frac{M(\infty)}{M_t}\right] \tag{64}$$

For the special case of a linear molecular weight calibration curve over the elution volume range of interest,

$$W(v) = F(v)\frac{D_2(\infty)D_1(\infty)}{D_2(t)D_1(t)} \exp\{-[D_2(\infty) - D_2(t)]v\} \tag{65}$$

From Eqs. (60) and (61), it can be seen that $W(v)$ is then an explicit function of the effective Mark-Houwink parameters ϵ_t and K_t obtained from the hydrodynamic volume fitting procedure.

The Fourier Transform Method

Recently, Tung (*12*) has used a numerical Fourier transform method for correcting observed chromatograms with a Gaussian instrument spreading shape function. The general shape function of Eq. (14) is readily adaptable to the Fourier transform method. Since the statistical coefficients h, μ_3, and μ_4 can be determined as a function of elution volume with narrow MWD standards, corrected chromatograms and subsequently corrected DMWD curves can be determined for broad as well as for narrow MWD samples. Following Tung's notation, the corrected chromatogram is given by

$$W(v) = (1/\sqrt{2\pi}) \int_{-\infty}^{\infty} [W_r(k) \cos(kv) + W_i(k) \sin(kv)]\, dk \quad (66)$$

where

$$W_r(k) = \frac{[F_r(k)G_r(k) + F_i(k)G_i(k)]}{\sqrt{2\pi}[G_r^2(k) + G_i^2(k)]} \quad (67)$$

$$W_i(k) = \frac{[F_i(k)G_r(k) - F_r(k)G_i(k)]}{\sqrt{2\pi}[G_r^2(k) + G_i^2(k)]} \quad (68)$$

The functions $F_r(k)$ and $F_i(k)$, and $G_r(k)$ and $G_i(k)$ refer to the real and imaginary parts of the Fourier transforms of the normalized observed chromatogram, $F(v)$, and the shape function $G(v)$, respectively. The functions $F_r(k)$ and $F_i(k)$ are evaluated numerically. The functions $G_r(k)$ and $G_i(k)$ can be obtained analytically. The Fourier transforms of $G(v - y)$ expressed in terms of the reduced variable $x = (v - y)h^{\frac{1}{2}}$ is

$$G(k) = (1/\sqrt{2\pi}) \int_{-\infty}^{\infty} G(x) \exp(ikx/\sqrt{h})\, dx \quad (69)$$

Through the use of the generating function (*20*) for Hermite polynomials, the exponential term in the integrand of Eq. (69) becomes

$$\exp(ikx/\sqrt{h}) = \exp(-k^2/2h) \sum_{n=0}^{\infty} \frac{H_n(x)}{n!} \left(\frac{ik}{\sqrt{h}}\right)^n \quad (70)$$

Substitution of Eqs. (70) and (21) into Eq. (69), along with the use of the ortho-normality conditions for Hermite functions as expressed by Eq. (24), leads to the following general expression for $G(k)$,

$$G(k) = (1/\sqrt{2\pi}) \exp(-k^2/2h) \left[1 + \sum_{n=3}^{\infty} \{(A_n/n!)(ik/h)^n\}\right] \quad (71)$$

Using the Edgeworth series (*24*) form of Eq. (14), where $A_5 = 0$ and $A_6 = 10A_3^2$ and $A_n = 0$ for $n \geq 7$, the expressions for $G_r(k)$ and $G_i(k)$ expressed in terms of h, μ_3, and μ_4 are

$$G_r(k) = (1/\sqrt{2\pi}) \exp(-k^2/2h) \left[1 + \left(\frac{\mu_4}{24} - \frac{1}{8h^2}\right)k^4 - \frac{1}{2}(\mu_3/6)^2 k^6\right] \quad (72)$$

$$G_i(k) = (1/\sqrt{2\pi}) \exp(-k^2/2h)[-(\mu_3/6)k^3] \quad (73)$$

Use of Eqs. (72) and (73) in Eqs. (66), (67), and (68) will lead to the corrected chromatogram $W(v)$. The use of the Fourier transform method

with the general shape function can be used for nonlinear as well as linear calibration curves. The application of this formalism to nonlinear calibration curves will be extensively discussed in Part II of this series.

CONCLUSIONS

A general analytical instrument spreading shape function containing statistical coefficients h, μ_3, and μ_4 has been proposed to correct GPC chromatograms for axial dispersion, skewing, and flattening. This shape function has been used to develop simple algebraic equations which correct $\bar{M}_n(\infty)$, $\bar{M}_w(\infty)$, and $[\eta](\infty)$ to their true values. Application of these correction equations to infinite resolution GPC data has yielded corrected values in reasonable agreement with the experimental absolute values. The parameters h and μ_3 may be determined from the observed chromatograms of characterized standards from either knowing $\bar{M}_n$ and $\bar{M}_w$ or knowing $\bar{M}_n$ and $[\eta]$. Determination of h, μ_3, and μ_4 requires knowledge of $\bar{M}_n$, $\bar{M}_w$, and $[\eta]$. The use of $\bar{M}_n$ and $[\eta]$ to determine h and μ_3 is of particular advantage for situations where the determination of $\bar{M}_w$ is not experimentally feasible.

The use of the hydrodynamic volume concept to fit for calibration and DMWD curves corrected for skewing and axial dispersion has been demonstrated. The potential use of the general instrument spreading shape function with the numerical Fourier transform method for correcting DMWD curves has been outlined. The general instrument spreading shape function should be readily adaptable to the correction methods of Smith (*3*); Pierce and Armonas (*6*); Pickett, Cantow, and Johnson (*5*); and the method of Chang and Huang (*10*) for correcting DMWD curves. This shape function also should have applicability to other areas of chromatography and to many fields of spectroscopy where it is important to accurately and analytically describe deviations from the Gaussian peak shape and separate overlapping skewed peaks (*30*, *31*).

Acknowledgments

The authors would like to acknowledge the contribution of Mr. Wilfred J. Renaudette in assisting the experimental GPC work, Mr. James H. Clark for his assistance in the GPC data reduction, and Mrs. C. M. Fraser and Miss L. Freeman for helpful assistance in the programming of some of the computer techniques in this work.

List of Symbols

A_n	the coefficients in the general shape function in Eq. (14)
A_3	coefficient of general shape function which is a statistical measure of skewness and defined by Eq. (16)
A_4	coefficient of general shape function which is a statistical measure of flatness and defined by Eq. (17)
$C(v_M)$	normalized chromatogram height at elution volume v_M
D_1, $D_1(\infty)$, D_2, $D_2(\infty)$	infinite resolution molecular weight vs counts calibration curve constants and defined by Eq. (6)
$D_1(t)$, $D_2(t)$	corrected molecular weight vs counts calibration curve constants
(da/dM)	DMWD function of molecular weight as defined by Eq. (54)
$[da/dM](\infty)$, $[da/dM](t)$	DMWD functions of molecular weight based on the infinite resolution and corrected molecular weight calibration curves, respectively
(da/dZ)	differential distribution of hydrodynamic volume as defined by Eq. (58)
$(df/dv)_{v_{M(\infty)}}$, $(df_t/dv)_{v_{M_t}}$, $(df'/dv)_{v_Z}$	slope of the infinite resolution molecular weight, corrected molecular weight and hydrodynamic volume calibration curves, respectively
DMWD	differential molecular weight distribution
$F(v)$	function describing normalized observed chromatogram heights at elution volume v
$\bar{F}$	bilateral Laplace transform of $F(v)$
$F_r(k)$, $F_i(k)$	real and imaginary parts of the Fourier transform of $F(v)$
$f(v)$	function describing infinite resolution molecular weight calibration curve at elution volume v

$f'(v)$	function describing infinite resolution hydrodynamic volume calibration curve at elution volume v
$f_t(v)$	function describing molecular weight calibration curve corrected for instrument spreading
$G(v - y)$, $G(x)$	general shape functions defined by Eqs. (14) and (21), respectively
$\bar{G}$	bilateral Laplace transform of $G(v - y)$
$G_T(v - y)$	normal form of the Gaussian instrument spreading function
$G_T^n(v - y)$	nth order derivatives of $G_T(v - y)$ with respect to v
$G_r(k)$, $G_i(k)$	real and imaginary parts of the Fourier transform of $G(v - y)$
$H_n(x)$	Hermite polynomials of order n
h, h'	resolution factors defined by Eqs. (18) and (39), respectively
k	Fourier transform variable
K, K_t	empirical and effective Mark-Houwink pre-exponential parameters, respectively
M, $M(v)$	molecular weight in calibration curve corresponding to ideal monodisperse species at elution volume v as defined by Eq. (6)
M_L, M_H	lowest and highest molecular weights of the sample, respectively
$M_k(\infty)$, $M_k(t)$	infinite resolution and absolute or corrected kth molecular weight average as defined by Eq. (4)
$\bar{M}_n$, $\bar{M}_n(t)$	true or absolute value of the number-average molecular weight
$\bar{M}_n(\infty)$	infinite resolution value of the number-average molecular weight
$\bar{M}_n(h)$, $\bar{M}_n(\mu_3)$, $\bar{M}_n(h,\mu_3)$, $\bar{M}_n(\mu_4)$, $\bar{M}_n(\mu_3,\mu_4)$	number-average molecular weights corrected for axial dispersion, skewing, axial dispersion and skewing, flattening, and skewing and flattening, respectively
M_t	molecular weight in corrected calibration curve as defined by Eq. (59)
$\bar{M}_v$	viscosity-average molecular weight

$\bar{M}_w$, $\bar{M}_w(t)$	true or absolute value of the weight-average molecular weight
$\bar{M}_w(\infty)$	infinite resolution value of the weight-average molecular weight
$\bar{M}_w(h)$, $\bar{M}_w(\mu_3)$, $\bar{M}_w(h,\mu_3)$, $\bar{M}_w(\mu_4)$, $\bar{M}_w(\mu_3,\mu_4)$	weight-average molecular weights corrected for axial dispersion, skewing, axial dispersion and skewing, flattening, and skewing and flattening, respectively
$M(\infty)$	infinite resolution molecular weight as defined by Eq. (6)
MWD	molecular weight distribution
m_2, m_3, m_4	calculated second, third, and fourth moments about the mean, respectively, of normalized observed chromatogram
P, $P(t)$	true or absolute value of polydispersity ratio $[\bar{M}_w(t)/\bar{M}_n(t)]$
$P(\infty)$	infinite resolution value of polydispersity ratio
$P(h,\mu_3)$, $P(\mu_3,\mu_4)$	polydispersity ratios corrected for axial dispersion and skewing, and skewing and flattening, respectively
PEV	peak elution volume
$R_n(t,\infty)$, $R_w(\infty,t)$, $R_v(\infty,t)$	the ratios $\bar{M}_n(t)/M_n(\infty)$, $M_w(\infty)/\bar{M}_w(t)$, and $[\eta](\infty)/[\eta](t)$, respectively
s	bilateral Laplace transform variable
sk	empirical skewing operator of Balke and Hamielec
v	elution volume
v_L, v_H	elution volumes corresponding to lowest and highest molecular weight of the sample, respectively
v_M	elution volume at molecular weight M
v_Z	elution volume at hydrodynamic volume Z
$W(v)$, $W(y)$	functions describing normalized corrected chromatogram height at elution volume v and y, respectively
$\bar{W}$	bilateral Laplace transform of W(v)
$W_r(k)$, $W_i(k)$	real and imaginary parts of the Fourier transform of W(v)

x	reduced dimensionless variable defined by equation (19)
y	elution volume y
Z	hydrodynamic volume as defined by Eq. (55)
Z_L, Z_H	lowest and highest hydrodynamic volume of the sample, respectively

Greek Letters

ϵ, ϵ_t	empirical and effective Mark-Houwink exponential parameters, respectively
$[\eta]$, $[\eta](t)$	true or absolute value of the intrinsic viscosity
$[\eta](\infty)$	infinite resolution value of the intrinsic viscosity
$[\eta](h)$, $[\eta](\mu_3)$, $[\eta](h,\mu_3)$, $[\eta](\mu_4)$, $[\eta](\mu_3,\mu_4)$	intrinsic viscosities corrected for axial dispersion, skewing, axial dispersion and skewing, flattening, and skewing and flattening, respectively
μ_2, μ_3, μ_4, μ_n	second, third, fourth, and nth order moments about elution volume of the instrument spreading function
$\phi(x)$	normal form of the Gaussian instrument spreading function in reduced variable notation
$\phi^n(x)$	nth order derivative of $\phi(x)$ with respect to x

REFERENCES

1. L. H. Tung, *J. Appl. Polym. Sci.*, **10**, 375 (1966).
2. J. H. Duerksen and A. E. Hamielec, *J. Polym. Sci., Part C*, **21**, 83 (1968).
3. W. N. Smith, *J. Appl. Polym. Sci.*, **11**, 639 (1967).
4. M. Hess and R. F. Kratz, *J. Polym. Sci., Part A-2*, **4**, 731 (1966).
5. H. E. Pickett, M. J. R. Cantow, and J. F. Johnson, *J. Polym. Sci., Part C*, **21**, 67 (1968).
6. P. E. Pierce and J. E. Armonas, *J. Polym. Sci., Part C*, **21**, 23 (1968).
7. L. H. Tung, J. C. Moore, and G. W. Knight, *J. Appl. Polym. Sci.*, **10**, 1261 (1966).
8. L. H. Tung, *J. Appl. Polym. Sci.*, **10**, 1271 (1966).
9. S. T. E. Aldhouse and D. M. Stanford, Paper presented at the 5th International GPC Seminar, London, May, 1968.

10. K. S. Chang and R. Y. M. Huang, *J. Appl. Polym. Sci.,* **13,** 1459 (1969).
11. S. T. Balke and A. E. Hamielec, *J. Appl. Polym. Sci.,* **13,** 1381 (1969).
12. L. H. Tung, *J. Appl. Polym. Sci.,* **13,** 775 (1969).
13. W. W. Yau, H. L. Suchan, and C. P. Malone, *J. Polym. Sci., Part A-2,* **6,** 1349 (1968).
14. H. E. Pickett, M. J. R. Cantow, and J. F. Johnson, *J. Appl. Polym. Sci.,* **10,** 917 (1966).
15. M. Freeman and P. P. Manning, *J. Polym. Sci., Part A,* **2,** 2017 (1964).
16. ArRo Laboratories, Inc., Private communication.
17. A. C. Aitken, *Statistical Mathematics,* Oliver and Boyd, Edinburg, 1962, pp. 64–66.
18. M. Abramowitz and I. A. Stegun, *Handbook of Mathematical Functions,* National Bureau of Standards Applied Mathematics Series 55, Washington, D.C. 1964, pp. 927–935.
19. R. S. Burington and D. C. May, *Handbook of Probability and Statistics,* Handbook Publishers, Sandusky, Ohio, 1953, pp. 91f.
20. H. Cramer, *Mathematical Methods of Statistics,* Princeton Univ. Press, Princeton, New Jersey, 1954, p. 133.
21. V. S. Pugachev, *Theory of Random Functions,* Addison-Wesley, New York, New York, 1962, pp. 44f.
22. H. Freeman, *Introduction to Statistical Inference,* Addison-Wesley, New York, New York, 1963, Chapter 18.
23. J. A. Greenwood and H. O. Hartley, *Guide to Tables in Mathematical Statistics,* Princeton Univ. Press, Princeton, New Jersey, 1962, pp. 407f.
24. D. E. Barton and K. E. Dennis, *Biometrika,* **39,** 425 (1952).
25. D. W. Marquardt, *J. Soc. Ind. Appl. Math.,* **2,** 431 (1963).
26. G. Meyerhoff, *J. Polymer Sci., Part C,* **21,** 31 (1968).
27. A. E. Hamielec, Published Lecture Notes from Two-Day Short Course in Gel Permeation Chromatography at Washington University, St. Louis, April 25–26, 1969.
28. Z. Grubisic, P. Rempp, and H. Benoit, *J. Polym. Sci., Part B,* **5,** 753 (1967).
29. H. Coll and L. R. Prusinowski, *J. Polym. Sci., Part B,* **5,** 1153 (1967).
30. E. Grushka, M. N. Myers, P. D. Schettler, and J. C. Giddings, *Anal. Chem.,* **41,** 889 (1969).
31. H. M. Gladney, B. F. Dowden, and J. D. Swalen, *Anal. Chem.,* **41,** 883 (1969).
32. A. H. Wachter and W. Simon, *Anal. Chem.,* **41,** 90 (1969).

Received by editor February 23, 1970